UNIVERSITY OF CALIFORNIA, MERCED

Critical behavior of interacting Brownian motions and Lévy flights.

A dissertation submitted in partial satisfaction of the

requirements for the degree Doctor of Philosophy

in Physics

by

Igor Goncharenko

Committee in charge:

Assistant Professor Linda S. Hirst, Chairman
Assistant Professor Ajay Gopinathan
Professor Michael E. Colvin
Professor Raymond Chiao
Assistant Professor Jay E. Sharping

2010

The dissertation of Igor Goncharenko is approved, and it is acceptable in quality and form for publication on microfilm:

_____

_____

_____

_____

_____

Chairman

University of California, Merced

2010

To my wife Inna

Contents

Signature Page iii

Dedication Page iv

Acknowledgements vii

Vita viii

Publications ix

Abstract x

1 Introduction **1**

1.1 Random walks and Lévy flights 3

1.2 Examples of Lévy flights 4

1.3 Field theories of random walks and Lévy flights 7

1.4 Vicious Walks 11

1.5 Encounters of interacting walks and Lévy flights: applications 13

1.6 Foundation of Renormalization Group 18

2 Vicious walks with long-range interactions **20**

2.1 Introduction 20

2.2 Modelling VW with long-range interations 23

2.3 The Renormalization of observables 29

2.4 Calculation of critical exponents and discussion 35

3 Vicious Lévy flights **42**

3.1 Introduction 42
3.2 RG flow equations and fixed points 43
3.3 Survival probability exponent computation 47
3.4 Comparison with numerical results and discussion 50

4 Conclusions **54**

5 Appendix **58**
5.1 Appendix A 58
5.2 Appendix B 60
5.3 Appendix C 61
5.4 Appendix D 64
References 66

Acknowledgements

I am grateful to my advisor Ajay Gopinathan for having suggested the topic of this thesis and for his constant scientific guidelines and encouragement.

Also I thank my wife Inna, to whom this thesis is dedicated, for her care and love.

Vita

26 October 1983	Born, Sverdlovsk, USSR
2005	B.S. in Physics, Moscow State Pedagogical University, Moscow, Russia
2007	M.S. in Physics, Peoples' Friendship University of Russia, Moscow, Russia
2010	Ph.D. in Physics, University of California, Merced

Publications

1. I. Goncharenko and A. Gopinathan, "Optimal Yield Rates in Enzymatic Reactions with Undesirable Intermediate States", proceedings of World Congress on Engineering and Computer Science, p.24 (2008)

2. I. Goncharenko and A. Gopinathan, "Optimal Kinetics for Chaperonin Assisted Protein Folding", IAENG Transactions on Engineering Technologies Volume II - p.13 (2008)

3. I. Goncharenko, M. Colvin and A. Gopinathan, "Optimal Nanocarrier Design for Cancer Cell Targeting", to be submitted to Science

4. I. Goncharenko, "Exact spectral dimension of the random surface", arXiv: 0908.3543, submitted to J Stat Mech

5. I. Goncharenko and A. Gopinathan, "Vicious walks with long-range interactions", Phys Rev E **82**, 011126 (2010), arXiv: 1003.5970

6. I. Goncharenko and A. Gopinathan, "Vicious Lévy flights", arXiv: 1007.2008, submitted to Phys Rev Lett

Abstract of the Dissertation

Critical behavior of interacting Brownian motions and Lévy flights.

by

Igor Goncharenko
Doctor of Philosophy in Physics
University of California, Merced, 2010
Assistant Professor Linda S. Hirst, Chairman

This dissertation studies the late-time critical behavior of interacting many-particle systems. Two examples of such systems considered here are Brownian vicious walks with long-range interactions and vicious Lévy flights.

In the first example we consider distinct groups of independent diffusive particles interacting by means of a long ranged potential that decays in d dimensions with distance r as r^{-d-s} such that the process is terminated upon the intersection of any two trajectories of particles in the spatio-temporal plane. The main characteristics of this system are the survival and reunion probabilities defined, respectively, as the probability that no trajectories intersect up to time t and the probability that all trajectories meet each other exactly at time t. We employ methods of renormalized

field theory to show that these quantities decay as $t^{-\alpha}$ and $t^{(N-1)d/2-2\alpha}$, respectively, where N is total number of particles. We calculate, for the first time, the exponent α for all values of parameters s and d to first order in the double expansion in $\varepsilon = 2-d$ and $\delta = 2-d-s$. We show that there are several regions in the $s-d$ plane corresponding to different scalings for survival and reunion probabilities. Furthermore, we calculate the leading logarithmic corrections, for the first time.

In the second example we study the statistics of encounters of Lévy flights by introducing the concept of vicious Lévy flights - distinct groups of walkers performing independent Lévy flights with the process terminating upon the first encounter between walkers of different groups. We show that the probability that the process survives up to time t decays as $t^{-\alpha}$ at late times. We compute α up to the second order in ε-expansion, where $\varepsilon = \sigma - d$, σ is the Lévy exponent and d is the spatial dimension. For $d = \sigma$, we find the exponent of the logarithmic decay exactly. Theoretical values of the exponents are confirmed by numerical simulations.

Chapter 1

Introduction

Understanding the behavior of non-equilibrium, interacting, diffusive, many-particle systems is a long standing problem in physics. The main motivation for studying such systems is that they exhibit critical behavior. More precisely, below the upper-critical dimension (when fluctuations become relevant or the correlation length becomes diverges) a large time scale emerges, which characterizes the time evolution of typical quantities defined through correlation functions (such as intersection probabilities). This phenomenon is called *critical slowing down*. It leads to universal behavior and dynamic scaling laws of time dependent quantities (macroscopic variables). A few examples of systems, where this phenomenon takes place, are reaction-diffusion problems [1] and kinetic Ising models [2, 3]. To study how physical observables behave under scale transformations we will use renormalization group (RG) methods [4]. RG is probably the most useful tool to do a systematic computation of the critical exponents that classify different universality classes. RG was first used in order to explain critical behavior of systems in thermal equilibrium. However, systems that are maintained out-of-equilibrium by some driven force also exhibit critical behavior, which can be analyzed by dynamic RG techniques [5]. In the initial formulation, these systems are represented in terms of stochastic partial differential equations (Langevin equations). It is well-known that there exists a well-established

mapping of stochastic partial differential equations to a field-theoretic representation [6]. This method relies on the introduction of second quantized creation-annihilation operators and then taking the appropriate continuum limit to yield a statistical path integral formulation. Starting with the field-theoretic formulation of the problem, the standard RG machinery can be implemented to compute universal quantities.

The main topic of this thesis is application of RG methods to study the statistics of encounters of

- Brownian motions with long-range interaction potential between particles,
- Lévy flights.

The thesis is organized as follows. The following section (1.1) provides a brief review of the properties of Brownian motions and Lévy flights. Since the concept of a Lévy flight is not as widely prevalent as Brownian motion, we give examples of real world systems that perform Lévy flights in Section 1.2. Section 1.3 describes the mapping of stochastic processes such as Brownian motion and Lévy flights onto field theories. The concept of vicious walks is introduced in Section 1.4 and a brief survey of physical applications is also presented. Examples of systems where vicious walks with long-range interactions and vicious Lévy flights - the two main topics of this thesis - naturally arise are considered in Section 1.5. Section 1.6 describes the foundation of the RG technique in the context of the vicious walk model. In chapter 2 we describe in detail, our solution to the vicious walks problem in the presence of long-range interactions between the walkers. In chapter 3 we describe how we solve the problem of vicious Lévy flights, where we allow the walkers to perform long-range jumps. Finally, in chapter 4, we give our conclusions and list open problems for future studies.

1.1 Random walks and Lévy flights

The main idea of classical physics is that, given initial conditions, trajectories of particles can be derived from the equation of motion unambiguously. The fundamental principle of quantum physics rejects this idea and forces us to speak about a probability distribution instead of a particle's trajectory. Descriptions in terms of probability distributions are also necessary in classical stochastic systems which are subjected to randomness in the form of noise. The most simple, but still non-trivial, example of such a process is the random walk. A random walk[1] is a sequence of independent identically distributed Bernoulli random variables ξ_i, i.e. $P(\xi_i = +1) = p$ and $P(\xi_i = -1) = q$, where $p + q = 1$. Physically this represents a particle performing a random walk in one dimension with probability p to go to the right and probability q to go to the left. If S_0 is the initial position of the random walk then the position S_k after k steps will be at $S_k = S_0 + \xi_1 + \ldots + \xi_k$. A sequence $(S_0, S_1, \ldots, S_k)$ is a path of the random walk. The statistical weight of the path connecting $S_0 = 0$ and $S_k = x$ on the one-dimensional regular lattice is

$$P_k(0, x) = p^{(k+x)/2} q^{(k-x)/2} C^k_{(k+x)/2}, \tag{1.1}$$

where $C^k_l = k!/[l!(l-k))!]$. In continuous space and time the corresponding quantity will be denoted as $P(0, 0; x, t)$ or as a matrix element $\langle 0|P(0, t)|x\rangle$. In this case the step length l is drawn from some probability distribution function $p(l)$. If the process is Markovian, space isotropic and translation-invariant and also $p(l)$ decays *at least* exponentially at long distances (locality) then one can derive the asymptotics of the

[1]The walk usually represents a sequence of jumps on the sites of a lattice. If one considers a similar process in continuous space then it is usually called Brownian motion.

conditional probability

$$P(0,0;x,t) \sim \frac{1}{(2\pi Dt)^{d/2}} \exp(-x^2/2Dt). \tag{1.2}$$

An important point to make is that the mean square displacement of a random walk grows linearly in time $\langle x^2(t)\rangle = Dt$. This kind of diffusion is called normal or Gaussian diffusion. If one relaxes the locality condition, i.e. instead of demanding exponential decay allow at least a power law decay, then we obtain a more general process - a Lévy flight. The characteristic function of the Lévy flight (Fourier transform of the conditional probability of the spatial distribution) is

$$\tilde{P}(k,t) = \exp(Dk^\sigma t), \tag{1.3}$$

where the constant σ is called the Lévy exponent. For $\sigma = 2$, we recover the Fourier image of the Gaussian distribution implying that we have normal diffusion. Direct inversion of (1.3) for values of $\sigma > 2$ will not give a positive probability distribution, but this is the consequence of the fact that the k^2 term becomes dominant over the k^σ term. Thus for $\sigma > 2$ one obtains a Gaussian distribution as well. Only values of $0 < \sigma < 2$ produce anomalous diffusion behavior. The mean square displacement of a Lévy flight grows faster than linear $\langle x^2(t)\rangle = Dt^{2/\sigma}$, since the ratio $2/\sigma$ is greater than one. Such dynamics is called superdiffusive.

1.2 Examples of Lévy flights

Diffusion or Brownian motion is ubiquitous in physics with well-known examples including heat, sound and light transport. Lévy flights on the contrary are less common. In an effort to make the reader more familiar with this process, we present three separate examples of real world processes governed by Lévy flights. These are human travel (sociology), DNA-binding proteins diffusion (biology), and

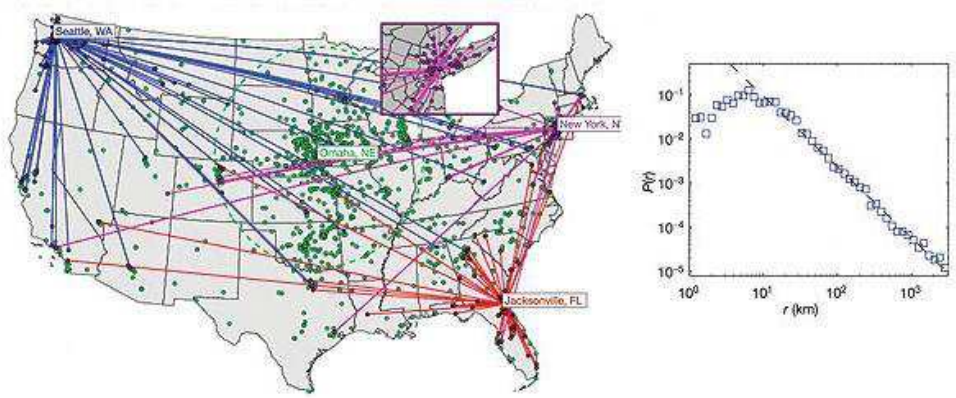

Figure 1.1: The probability distribution $P(r)$ of traveling a distance r ($\sigma = 0.59$) [7].

light wave propagation in novel optical material (physics).

We first consider the case of human travel. It has been shown that statistically reliable quantitative assessment of human movements can be tracked by observing the spread of half a million one dollar bank note bills across the country [7]. Analysis of the spread of dollar bills showed that the distribution of traveling distances decays as a power law $P(r) \sim r^{-1-\sigma}$, indicating Lévy flight behavior. Thus travel patterns can be described by a combination of frequent short distance travels interspersed with a few long distance ventures. Figure 1.1 shows the short-time (traveling time less than 14 days) trajectories of one dollar bills originating from different places. The linear function in the log-log scale indicates a power law behavior and a Lévy exponent is evaluated from the slope of this line.

The diffusion of DNA-binding proteins such as transcription factors is another example of Lévy flight behavior [8]. It is known that after initial non-specific binding to the DNA, the protein starts to search for the target binding site by performing a random walk on the one dimensional DNA strand. In addition, by taking advantage of DNA looping, some proteins may accelerate their search by making inter-segmental

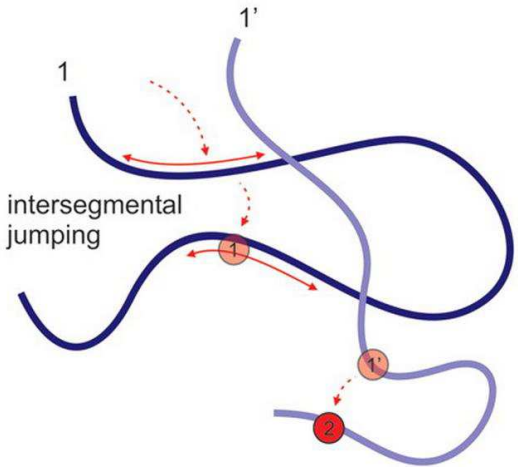

Figure 1.2: On coiled DNA the enzyme can be captured by a segment it has not yet visited, leading to an intersegmental jump [8].

jumps (see Figure 1.2). This process can be treated as a simple diffusion on a regular one dimensional lattice supplied with random long-range links. The emergent structure then produces a small-world network. If the distribution of the random links is distance dependent and decays as a power law $r^{-1-\sigma}$, where r is Euclidean distance on the regular lattice, then the resulting motion is equivalent to a Lévy flight. DNA looping is governed by polymer statistics which indeed predicts a power law distribution of loop sizes and hence jump lengths.

Our third example is light transport in optical materials with impurities [9]. Here the density of titanium dioxide scatterers was modulated by suspending microspheres of different diameters d chosen from a distribution $d^{-2-\sigma}$ in liquid Sodium Silicate ($SiO_2 : NaOH$). It was found that in such materials the transmission of light has Lévy Flight statistics with a Lévy exponent σ. This was shown experimentally by measuring the intensity of the light that scatters through slabs of different thicknesses. Figure 1.3 shows the transmission as a function of sample's thickness. Moreover if the diameters of the suspended microspheres are all identical, then one recovers normal (Gaussian) transmission decay.

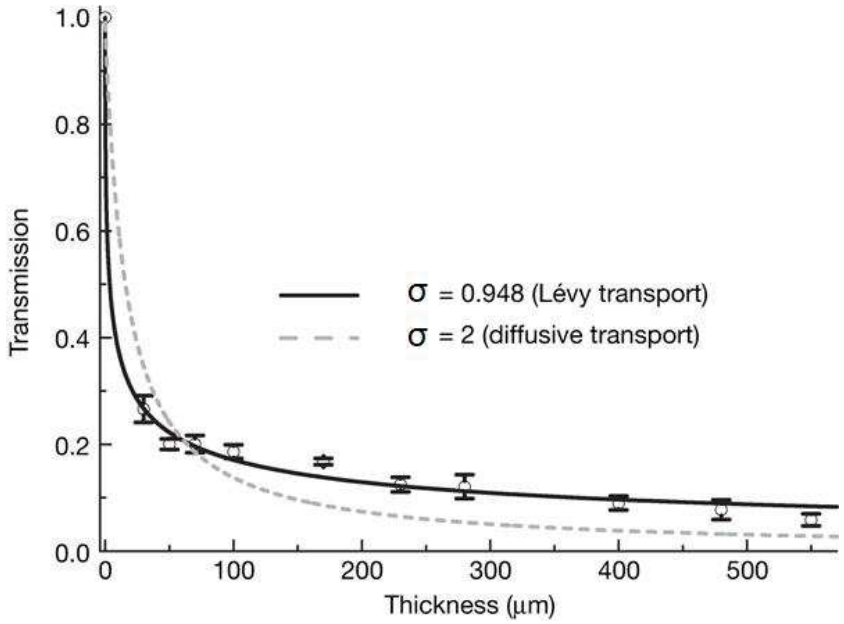

Figure 1.3: Transmission (intensity distribution) decays as a power law with a Lévy exponent $\sigma = 0.95$ [9].

Thus Lévy flights arise in a variety of different contexts and are an important subset of random walks in general.

1.3 Field theories of random walks and Lévy flights

Here we give a brief introduction on how stochastic processes can be mapped to field theories. From section 1.1, it is manifest that one can associate the matrix element of a random walk with the path integral

$$\langle 0|P(0,t)|x\rangle = \int \mathrm{D}x \exp(\int_0^t \dot{x}^2(\tau)/2D d\tau). \tag{1.4}$$

since the left and right hand sides of the equation (1.4) coincide with equation (1.1). Therefore a random walk can be treated as a free quantum particle. If one adds an interaction term $V(x)$ to the kinetic energy term in the exponent in (1.4) then the problem of finding this integral is equivalent to studying the scattering of a particle

under the external potential $V(x)$. The scattering amplitude can be found using the Born approximation. Although quantum mechanics can be treated as a zero-dimensional quantum field theory, we do not know how, using (1.4), one can derive a consistent field-theoretic path integral. Nevertheless, it is possible to construct such path integrals using other methods [10, 11].

We can start describing the state of the system with occupation numbers $|n_i(x)\rangle$, where x denotes a site on the discrete regular lattice and n_i is the number of particles of type i at that site. The dynamics of a random walk can be rewritten in terms of quantum mechanical creation and annihilation operators by making a correspondence between the lattice site occupation numbers $|n_i(x)\rangle$ and quantum harmonic oscillator eigenstates. Creation and annihilation operators are introduced for each lattice site, and are defined to obey the bosonic commutation relations

$$[a_i(x), a_j^\dagger(x')] = \delta_{ij}\delta(x - x'), \quad [a_i(x), a_j(x')] = [a_i^\dagger(x), a_j^\dagger(x')] = 0. \tag{1.5}$$

Defining the vacuum $|0\rangle$ by the equations $a_i(x)|0\rangle = 0$ for all i and x, we construct the basis of the Fock space $F = \otimes_x F_x$ as

$$|n_i(x)\rangle = \prod_x \prod_{i=1}^{p} a_i^{\dagger n_i(x)}(x)|0\rangle, \tag{1.6}$$

where index x runs over all sites of a regular lattice and i counts different types of boson-like particles. The state of the system is a vector in $\otimes_x F_x$

$$|\Psi(t)\rangle = \sum_{\{n_i(x)\}} P(\{n_i(x)\}, t)|n_i(x)\rangle, \tag{1.7}$$

where $P(\{n_i(x)\}, t)$, associated with the amplitude $\langle n_i(x)|\Psi(t)\rangle$, is interpreted as the probability for the system being in state $|n_i(x)\rangle$. For simple diffusion the Hamiltonian

can be written as

$$H = \sum_{i=1}^{p} \sum_{(x,x')} (a_i^\dagger(x) - a_i^\dagger(x'))(a_i(x) - a_i(x')), \tag{1.8}$$

where (x, x') means the summation over all neighboring pairs and index i enumerates different types of random walks. Thus, the state $|\Psi(t)\rangle$ is the solution of the Shrödinger equation

$$-\frac{\partial}{\partial t}|\Psi(t)\rangle = H|\Psi(t)\rangle, \quad |\Psi(t)\rangle = \exp(-Ht)|\Psi(0)\rangle. \tag{1.9}$$

Expectation value of any observable $\langle G(t)\rangle$ can be computed with the formula:

$$\langle G(t)\rangle = \langle 0|G|\Psi(t)\rangle. \tag{1.10}$$

We now derive the path integral form of (1.10). We introduce coherent states, representing a displaced vacuum state of the Fock space, such that

$$|\phi_i\rangle = \exp(-|\phi_i|^2/2 + \phi_i a_i^\dagger)|0\rangle. \tag{1.11}$$

The resolution of the identity can be written as an integral

$$1 = \int \frac{d^2\phi_i}{\pi} |\phi_i\rangle\langle\phi_i| \tag{1.12}$$

for each i. Dividing the time interval into small intervals and utilizing (1.12) one can infer that the expectation value in (1.10) can be equivalently rewritten as

$$G(t) = \lim_{\Delta t \to 0} \int \prod_i \prod_\tau d^2\phi_i(\tau) \langle 0|G|\phi_i(t)\rangle \times$$

$$\times \langle \phi_i(t)| \exp(H\Delta t)|\phi_i(t-\Delta t)\rangle \dots \langle \phi_i(\Delta t)| \exp(H\Delta t)|\phi_i(0)\rangle \langle \phi_i(0)|\Psi(0)\rangle. \tag{1.13}$$

We note that since Δt is infinitesimally small, we get

$$\langle\phi_i(\tau)|\exp(H\Delta t)|\phi_i(\tau-\Delta t)\rangle = \langle\phi_i(\tau)|\phi_i(\tau-\Delta t)\rangle\exp(H\Delta t), \tag{1.14}$$

where $H = H(\phi^\dagger(\tau), \phi(\tau-\Delta t))$ and the propagator can be rewritten using the definition of the coherent states

$$\langle\phi_i(\tau)|\phi_i(\tau-\Delta t)\rangle = \exp(\phi_i^\dagger(\tau)(\phi_i(\tau)-\phi_i(\tau-\Delta t)))\exp(|\phi_i(\tau)|^2/2-|\phi_i(\tau-\Delta t)|^2/2) \tag{1.15}$$

It is clear that the first exponent contains the time derivative in the limit $\Delta t \to 0$, so one can write

$$\phi^\dagger(\tau)(\phi(\tau)-\phi(\tau-\Delta t)) \sim \phi^\dagger\partial_t\phi\Delta t. \tag{1.16}$$

Since we are multiplying $\langle\phi(\tau)|\phi(\tau-\Delta t)\rangle$ for all τ, the squared terms from the second exponent will all cancel with each other. Thus we have proved that

$$\langle G(t)\rangle = \int(\prod_i \mathrm{D}\phi_i^\dagger\mathrm{D}\phi_i)G(\phi^\dagger,\phi)\exp(\phi^\dagger\partial_t\phi + H(\phi^\dagger,\phi)) \tag{1.17}$$

where the measure is defined as $\mathrm{D}\phi_i^\dagger\mathrm{D}\phi_i = \prod_\tau d^2\phi_i(\tau)$ and the evolution operator $H(\phi^\dagger,\phi)$ is obtained from (1.8). In the continuum limit the Hamiltonian is given by the formula

$$H(\phi^\dagger,\phi) = \sum_i D_i\phi_i^\dagger\nabla^2\phi_i, \tag{1.18}$$

where D_i plays the role of diffusion constant for particles of type i. Generalization to the case of Lévy flights is done by adding a fractional derivative term into the free Hamiltonian [12, 13]

$$H(\phi^\dagger,\phi) = \sum_i \left(D_i\phi_i^\dagger\nabla^2\phi_i + \tilde{D}_i\phi_i^\dagger\nabla^\sigma\phi_i\right). \tag{1.19}$$

1.4 Vicious Walks

Vicious walks (VW) represent a system of independent random walks such that any pair of walks occupying the same site at the same time annihilate each other and the process is terminated. The main motivation to consider such a system is that space-time trajectories of one dimensional vicious walks can be treated as fluctuating domain walls separating different phases of two-dimensional systems. It was first noted by M. E. Fisher [14]. Several questions can be addressed in the context of this model. What is the probability that all walkers survive for time t? What is the probability of a reunion of all walkers at some point x after time t? What is the probability of a reunion of all walkers anywhere after time t? The principal results are that the probability $S(t)$ that walkers survive for time t decays asymptotically as $S(t) \sim t^{-\alpha}$. If one knows the decay exponent α of the survival probability then the reunion and reunion anywhere exponents can be found by the formulas

$$\alpha_R = \frac{Nd}{2} + 2\alpha, \quad \alpha_{Ra} = \frac{(N-1)d}{2} + 2\alpha, \tag{1.20}$$

respectively, where N is the total number of walks and d is dimensionality of the space. Fisher found α exactly for N equivalent vicious walks in one dimension with the result:

$$\alpha = N(N-1)/4. \tag{1.21}$$

This exponent is called the Fisher exponent. We give one particular example of how it can be used in studying the two-dimensional Ising model. We will show that the decay of correlations for the zero field Ising model below the critical temperature T_c is determined by the decay exponent of the reunion probability of two vicious walks, α_R, in one dimension. The exact calculations show that the two-point correlation

function below T_c obeys the anomalous decay law

$$\langle s(0,0)s(x,y)\rangle = C(x,y) \sim r^{-2}, \tag{1.22}$$

where r is the Euclidean distance from $(0,0)$ to (x,y). Low-temperature expansions for Ising models are constructed by turning over spins from the one state to another state. One thus discovers that contributions to the two-point correlation function, $C(x,y)$, arise only from configurations in which both sites $(0,0)$ and (x,y) are linked by a chain of neighboring overturned spins so that they make an cluster (island) of opposite spins. The energy of such a configuration in zero field is determined solely by the total length of the perimeter of such a cluster. On the other hand, the perimeter of the cluster of spins can be associated with the statistical weight of the reunion of two vicious walks. Combining (1.20) with (1.21) one has that $\alpha_R = 2/2 + 2 \cdot 2/4 = 2$, which is in agreement with (1.22). Therefore the two-point correlation function of two-dimensional Ising model is in one-to-one correspondence with reunion probability of two vicious walks in one dimension.

Exact solutions such as (1.21) can not be obtained for more complicated cases of several groups of walks where members of each group are only vicious to members of other groups. RG is a method that can be useful for deriving analytical results for such systems. In order to derive the field theory of vicious walks, one uses the fact that the intersections are prohibited. This means that one can add local interactions of the form $\lambda_{ij}\phi_i^\dagger(x,t)\phi_i(x,t)\phi_j^\dagger(x,t)\phi_j(x,t)$ for $i \neq j$ between members of different groups and impose the condition $\lambda_{ij} \to \infty$. The Hamiltonian will then be [15]:

$$H(\phi^\dagger,\phi) = \sum_i D_i\phi_i^\dagger\nabla^2\phi_i + \sum_{i<j}\lambda_{ij}\phi_i^\dagger\phi_i\phi_j^\dagger\phi_j. \tag{1.23}$$

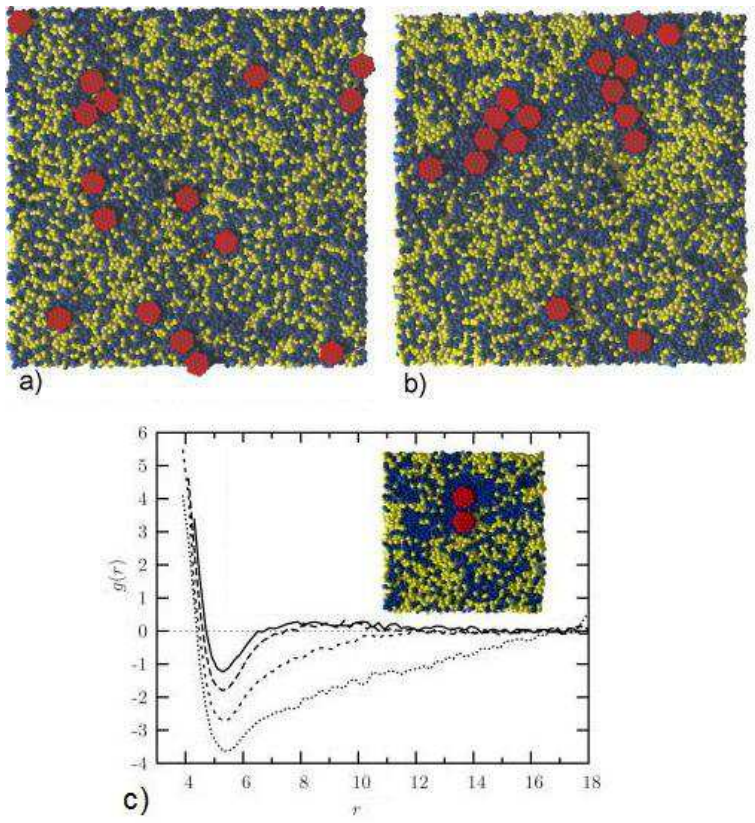

Figure 1.4: a) and b) are two top-view snapshots of the membrane showing the result of the aggregation of 16 proteins into clusters. c) Pair potentials $g(r)$ between two proteins as a function of separation r for different type proteins [17]. They mimic a Liénard-Wiechert potential $\sim (b/r)^{12} + (b/r)^6$.

1.5 Encounters of interacting walks and Lévy flights: applications

In the previous section we illustrated how vicious walks arise in a variety of physical contexts. The statistics of encounters between freely diffusing walkers was the fundamental quantity of interest. However in many systems one might be interested in encounters between walkers that have long range interactions with each other or encounters between walkers that perform long range hops. It is particularly important to understand these statistics when the encounters can affect the outcome

of the process in question. In this section, we present several real world examples of processes, where the study of encounters between either interacting walkers or Lévy flights are critically important to understanding the process.

We start with examples for vicious walks with long-range interactions. We first consider the diffusion of membrane-protein inclusions [16, 17]. Protein aggregation on the cell (lipid bilayer) membrane determines many biological functions including intracellular transport and signaling [18]. A protein that is bound to the cell surface, can exhibit Brownian-like dynamics along the membrane. Typical proteins explore an area of approximately 20 μm^2 every second [19]. They can meet with other proteins and create new mobile domains or rafts (see Figure 1.4, a and b). When an isolated protein binds to the cell membrane, then the membrane remodels itself creating a curvature or a deformation. When two or more such proteins are relatively close (far enough for protein-protein interaction to be negligible but close enough that induced membrane deformations can overlap with each other) it creates a long-range interaction potential between proteins (see Figure 1.4, c). An important quantity describing the dynamics of this system is the average time it takes for any two proteins to find each other. It is manifest that it should depend on the interaction potential between the proteins. Thus the system of diffusive membrane inclusions can be modeled as a system of vicious walks with long-range interaction and the statistics of encounters between proteins, which is important for signaling and endocytosis, is determined by the survival probability of vicious walks.

Next, we consider exciton-exciton annihilation in carbon nanotubes [20]. Quasi one dimensional carbon nanotubes (see Figure 1.5, a) are promising candidates to replace conventional metal wires in electronic circuits [21]. The unique electronic properties of these structures allow an increase in the maximum current density by several orders of magnitude providing a huge increase in computational

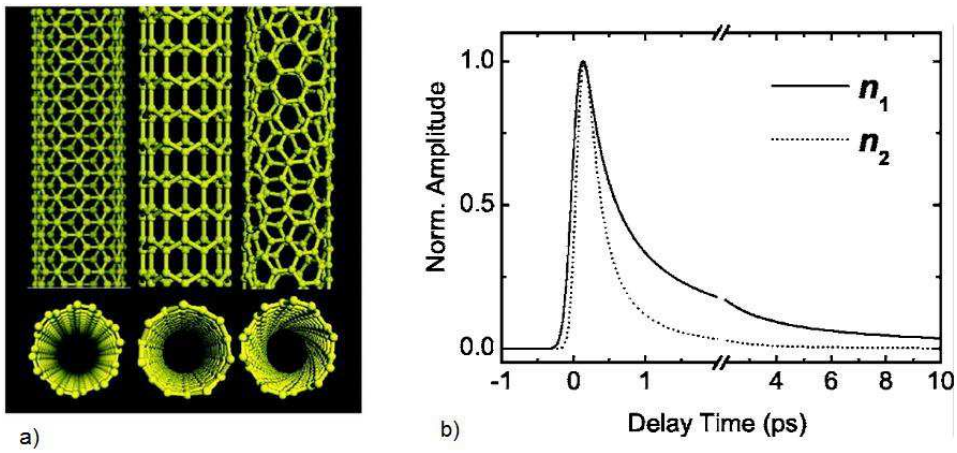

Figure 1.5: a) Schematic illustrations of the structures of different SWNTs. b) The time evolution of two populations of the excitonic states. The data are normalized at the maximum populations [20].

power of computers that are made with such electronic circuits. Physically, semiconducting characteristics of the nanotube are determined by the dynamics of excitons. Excitons are formed of one electron and one hole coupled together. In particular, observation of ultrafast relaxation of excitons in single walled carbon nanotubes (SWNT) (see Figure 1.5, b) showed that the diffusion-limited migration of excitons and exciton-exciton long-range interactions leave an imprint on the resulting time decay of the density of excitons. This dynamics is determined by the time that two excitations need to find each other in the system. Thus the annihilation process is conceptually similar to dynamics of a system of vicious walks with long-range interactions. The main quantity of interest, the survival probability that no two walks have found each other up to time t, is related to the annihilation rate of excitons. It decays as a power-law with time, which is the consequence of the fact that the process is diffusion limited. The decay exponent is sensitive to the dimensionality of the system and the interaction potential between excitons. This exponent describes the nature of the relaxation channels in several specific semiconducting nanotubes.

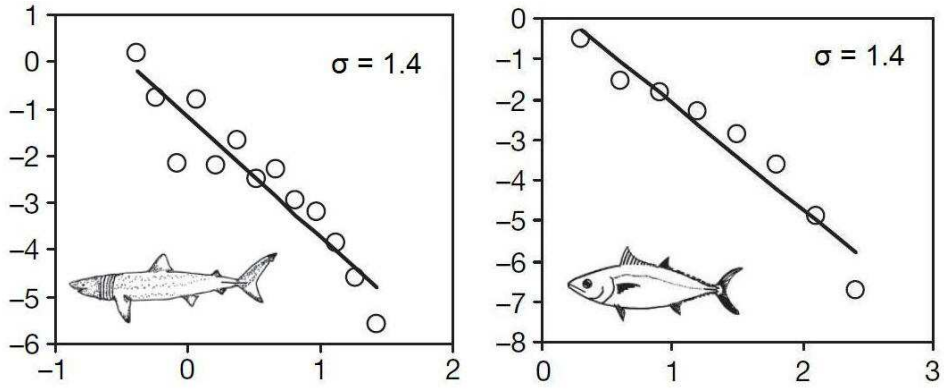

Figure 1.6: The probability distribution $P(r)$ versus size of the step r for shark and tuna ($\sigma = 1.4$) [22].

Thus vicious walks provide an important step towards a theoretical understanding of fast excitation kinetics in SWNT.

We now switch to describing systems where encounters of Lévy flights are critical. Consider marine animals searching for prey [22]. On large distance scales, marine animals are blind food foragers. However, contrary to the simple diffusive behavior one might expect, their search patterns are amazingly well described by Lévy flights. Figure 1.6 shows the log-log plot of frequency (probability distribution) $P(r)$ versus the length of vertical (depth) one-dimensional movements r for shark and tuna respectively. It is clear that $\log P(r)$ is linear in $\log r$ implying a Lévy type power-law decay $P(r) \sim r^{-1-\sigma}$. Lévy exponents are extracted from the slopes of the lines of each graph. It is clear that for different hunting strategies there will be different average times to catch the prey. The success of the search strategy can be quantitatively described by the the probability of a first lethal encounter between members of different populations, say shark and tuna. Since the shark and tuna are "vicious" to each other, we are clearly interested in the survival probability of vicious walks performing Lévy flights.

Similar considerations can be made for spider monkeys [23]. There is ev-

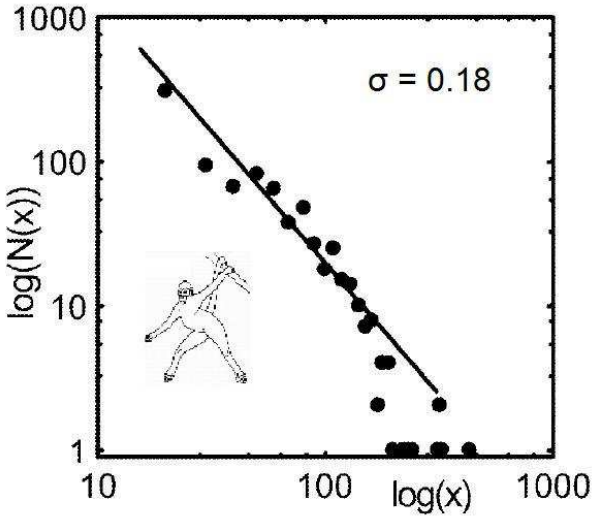

Figure 1.7: The probability distribution $P(r)$ versus size of the step r for spider monkey ($\sigma = 0.18$) [23].

idence that the daily movements of spider monkeys foraging for food (fruit trees) in the rain forest resemble two dimensional Lévy flights. Analyzing the short time (5min) movements of 20 spider monkeys it was shown that the probability $P(r)$ of taking a step of length r decays as $P(r) \sim r^{-2-\sigma}$, where the Lévy exponent is $\sigma = 0.18$ (see Figure 1.7). Male spider monkeys are not independent of each other. At the boundaries of their territory, males engage in very aggressive encounters with neighboring males. Thus one may treat the system of foraging spider monkeys as vicious Lévy flights. The survival probability of this system then translates into the probability that no fights have broken out upto a certain time.

The examples we have listed here constitute only a small sampling of the large variety of systems that can be modeled as either vicious walks with long range interactions or vicious Lévy flights. They do however demonstrate the breadth of disciplines to which our results may be applied.

1.6 Foundation of Renormalization Group

In this section, we present a self-contained description of the theory leading upto RG calculations in the context of vicious walk field theories. It is enough to consider the simplest situation of two Gaussian vicious walks to demonstrate the method. The action is

$$S = \int d^d x \int dt \left(\phi_1^\dagger \partial_t \phi_1 + D_1 \phi_1^\dagger \nabla^2 \phi_1 + \phi_2^\dagger \partial_t \phi_2 + D_2 \phi_2^\dagger \nabla^2 \phi_2 + \lambda \phi_1^\dagger \phi_1 \phi_2^\dagger \phi_2 \right). \quad (1.24)$$

It depends on 4 functionally independent fields. Our goal is to evaluate path integrals like (1.17). The simplest example of such an integral is the partition function

$$Z = \int \mathrm{D}\phi^\dagger \mathrm{D}\phi \exp\left(S[\phi^\dagger, \phi] \right), \quad (1.25)$$

which can be found using the steepest descent method. Therefore at the one-loop order an effective action [24, 25] can be written as

$$\Gamma_1(\phi^\dagger, \phi) = \frac{1}{2} \mathrm{tr} \ln \frac{\delta^2 S}{\delta\{\phi, \phi^\dagger\}_x \delta\{\phi, \phi^\dagger\}_y} \quad (1.26)$$

where $\delta\{\phi, \phi^\dagger\}_x$ denotes either $\delta\phi_i(x)$ or $\delta\phi_i^\dagger(x)$. Thus an effective action is a 4×4 matrix of hermitian operators. One example of taking these functional derivatives is

$$\frac{1}{2} \frac{\delta^2 S}{\delta\phi_1^\dagger(t,x)\delta\phi_1(t',y)} = G(t-t', x-y) + \lambda \phi_2^\dagger(t,x)\phi_2(t,x)\delta(t-t')\delta(x-y), \quad (1.27)$$

where $G(t,x)$ represents a second order differential operator of the theory or the propagator $G(x,t) = \langle \phi^\dagger(t,x)\phi(0,0) \rangle$. Its explicit form can be found using the time and space Fourier transform:

$$\int d^d x \int dt \phi^\dagger(t,x)(\partial_t + D\nabla^2)\phi(t,x) = \int dk d\omega \phi^\dagger(-\omega, -k)(\omega + Dk^2)\phi(\omega, k) \quad (1.28)$$

Thus the Fourier transform of the propagator reads $G(\omega, k) = (\omega + Dk^2)^{-1}$. Diagonalizing the fields in the action one derives the following expression

$$\Gamma_1(\phi^\dagger, \phi) - \Gamma_1(0,0) = \frac{1}{2}\mathrm{tr}\ln(1+K), \tag{1.29}$$

where K is the result of taking functionals derivatives (see (1.27)). Expanding the logarithm we obtain 1-loop contributions to correlation functions of the theory. The n-th order term corresponds to the 2n-point function.

The explicit calculation leads to the result:

$$\Gamma_1(\phi^\dagger, \phi) - \Gamma_1(0,0) = G_1(0,0)\int dt d^d x \phi_1^\dagger(x)\phi_1(x) + G_2(0,0)\int dt d^d x \phi_2^\dagger(x)\phi_2(x)$$

$$\int dt dt' d^d x d^d y \phi_1^\dagger(x)\phi_1(x) G_1(t-t', x-y) G_2(t'-t, y-x)\phi_2^\dagger(y)\phi_2(y) \tag{1.30}$$

where $G_i(\omega, k) = \omega + D_i k^2$. This expression allows us to explicitly write down the one-loop corrections to the 4-point correlation function for zero external momenta:

$$I_1 = \int \frac{d^d k d\omega'}{(\omega' + D_1 k^2)(\omega - \omega' + D_2 k^2)} = \int \frac{d^d k}{\omega + (D_1 + D_2)k^2} \tag{1.31}$$

When the dimension of space, d, is less then the upper-critical dimension d_c such integrals dverge. The goal of RG is to renormalize coupling constants such that these unphysical singularities $\sim \varepsilon^{-1}$ disappear in the computation of the other correlation functions.

Chapter 2

Vicious walks with long-range interactions

2.1 Introduction

Systems consisting of diffusing particles or random walks interacting by means of a long-range potential are non-equilibrium systems, which describe different phenomena in physics, chemistry and biology. From a physical perspective they are used to study metastable supercooled liquids [26, 27], melting in type-II high-temperature superconductors [28], electron transport in quasi-one-dimensional conductors [29] and carbon nanotubes [30]. From a chemical viewpoint the interest in these systems lies in the fact that some diffusion-controlled reactions processes rely on the diffusion of long-range interacting particles which react after they are closer than an effective capture distance. Some examples include radiolysis in liquids [31], electronic energy transfer reactions [32] and a large variety of chemical reactions in amorphous media [33]. From a biological viewpoint, the investigation of these systems is helpful in understanding the dynamics of interacting populations in terms of predator-prey models [34, 35, 36] and membrane inclusions with curvature-mediated interactions [16, 17].

Vicious walks (VW) are a class of non-intersecting random walks, where the

process is terminated upon the first encounter between walkers [14]. The fundamental physical quantity describing VW is the survival probability which is defined as the probability that no pair of particles has collided up to time t. Diffusing particles or walks that are not allowed to meet each other but otherwise remain free, we call pure VW. The behavior of pure VW is generally well-known. The survival probability for such a system has been computed in the framework of renormalization group theory in arbitrary spatial dimensions up to two-loop order [15, 37, 38]. These approximations have been confirmed by exact results available in one dimension from the solution of the boundary problem of the Fokker-Plank equation [34, 36], using matrix model formalism [46] and Bethe ansatz technique [39]. On the other hand the effect of long range interactions has been extensively investigated in many-body problems. It has been shown that the existence of long-range disorder leads to a rich phase diagram with interesting crossover effects [40, 41, 42]. If the potential is Coulomb-like ($\sim r^{-1-\sigma}$) then systems in one dimension behave similar to a one-dimensional version of a Wigner crystal [43] for $\sigma < 0$ and similar to a Luttinger liquid for $\sigma \geq 0$ [44]. If the potential is logarithmic then in the long-time limit the dynamics of particles are described by non-intersecting paths [45, 46]. The generalization of VW that includes the effect of long range interactions has not attracted much attention in the literature. Up to our knowledge there was one attempt to study long-range VW [47]. Here the authors considered the case of a long-range potential decaying as $gr^{-\sigma-d}$, where g is a coupling constant. It was shown by applying the Wilson momentum shell renormalization group that only one of the critical exponents characterize long-range VW. For a specific value of σ ($\sigma = 2 - d$) they show that the exponent γ, which determines the decay of the asymptotic survival probability with

time, is given by the expression:

$$\gamma = \frac{p(p-1)}{4} u_1, \tag{2.1}$$

where p the number of VW in the system, $u_1 = (\varepsilon/2 + [(\varepsilon/2)^2 + g]^{1/2})$ and $\varepsilon = 2 - d$. There are limitations to the above approach. First, it is restricted to a single form of the potential ($\sim r^{-2}$) and systems such as membrane inclusions and chemical reactions have different power-law potentials. Second, it considers identical walkers but one would like to have results if the diffusion constant of all walkers are different. Finally it is not convenient to compute higher-loop corrections using the Wilson formalism.

In this chapter we reconsider the problem of long-range VW using methods of Callan-Symanzyk renormalized field theory in conjunction with an expansion in $\varepsilon = 2-d$ and $\delta = 2-d-\sigma$. We note that it is more convenient to compute logarithmic and higher loop corrections by using this method. We derive the asymptotics of the survival and reunion probability for all values of the parameters (σ, d) for the first time.

In this chapter we will show that there are several regions in $\sigma - d$ plane in which we have different behavior of the critical exponent. Our results are summarized in Table 2.1. We note that results on the line $\sigma+d = 2$ have been obtained before [47]. Regions I and IV correspond to Gaussian or mean-field behavior (see Figure 2.3). In region II we found that the system reproduces pure VW. Logarithmic corrections in region III and at the short-range upper critical dimension $d = 2$ have been obtained as series expansion in $\delta = 2 - \sigma - d$.

The remainder of this chapter is organized as follows: Section 2.2 reviews the field theoretic formulation of long range VW and describes Feynman rules and dimensionalities of various quantities. In section 2.3 we derive the value of all fixed

Table 2.1: One-loop survival probability of p sets of particles with n_j particles in each set large-time asymptotic at different regions of the $\sigma - d$ plane. We refer to Figure 2.3 for specific value of σ and d in each region.

Region	Survival probability
I	$t^{-(d-2)/2} + t^{-(d+\sigma-2)/2}$
II	$t^{-\frac{1}{2}\sum_{ij} n_i n_j \varepsilon}$
III	$t^{-\frac{u_1}{2}\sum_{ij} n_i n_j (1+\delta/2 \ln t)}$
IV	$t^{-(d-2)/2}$
V, $d = 2$	$t^{-\frac{\sqrt{g_0}}{2}\sum_{ij} n_i n_j (1+\delta/2 \ln t)}$
VI, $\sigma = 2 - d$	$t^{-\frac{u_1}{2}\sum_{ij} n_i n_j}$

points and study their stability. Section 2.4 presents results for the critical exponents and logarithmic corrections of various dynamical observables. In Appendix A we give the details of the computation of some integrals that appear in Section 2.3.

2.2 Modelling VW with long-range interations

As the starting point of the description of our model we consider p sets of diffusing particles or random walks with n_i particles in each set $i = 1 \dots p$, with a pairwise intraset interaction which includes a local or short-range part and a non-local or long-range tail. The local part determines the vicious nature of particles: if two walks belonging to the different sets are brought close to each other, both are annihilated. Particles belonging to the same set are supposed to be independent. At $t = 0$ all particles start in the vicinity of the origin. We are interested in the survival and reunion probabilities of walks at time $t > 0$.

A continuum description of a system of N Brownian particles X_i with two-body interactions is simplified by the coarse-graining procedure in which a large number of microscopic degrees of freedom are averaged out. Their influence is simply modelled as a Gaussian noise-term in the Langevin equations. A convenient starting point for the description of the stochastic dynamics is the path-integral formalism. Then the system under consideration is modeled by the classical action

$$S = \int_0^{+\infty} dt \left(\sum_{i=1}^{N} \dot{X}_i^2/(2D_i) + \sum_{i<j} V(X_i - X_j) \right) \tag{2.2}$$

where t is (imaginary-)time, $X_i(t)$ is the d-dimensional vector denoting the position of ith particle at time t. D_i is an ith particle diffusion coefficient. The path-integral representation of the probability density function for the particle displacements from their original positions is given by the functional $\mathcal{Z} = \int \mathcal{D}X \exp[-S]$. The survival probability is defined as the expectation value

$$P(t) = \langle \prod_{i,j} [1 - \delta(X_i(t) - X_j(t))] \rangle \tag{2.3}$$

with respect to the functional $\mathcal{Z}$. It is computed in the framework of usual perturbation theory and will be a sum of integrals over internal degrees of freedom. It is more convenient to perform these integrations in Fourier space. To do this we would need the Fourier transform of the interaction potential $V(r)$. We note that it is comprised of a short-range part of the form $V_0(r) = \lambda\delta(r)$ and a long-range part which decays with the distance r as a power law, $V_l(r) = gr^{-d-\sigma}$. The Fourier transform of the latter is divergent if $\sigma \geq 0$. We introduce the cut-off parameter a to regularize the singularity $V_l(r) = g(r^2+a^2)^{-(d+\sigma)/2}$. Fourier transformation of this function is given by the expression

$$V_l(q) = g\frac{\pi^{d/2}2^{\sigma}}{\Gamma(\frac{d+\sigma}{2})}(q/a)^{\sigma/2}K_{\sigma/2}(aq), \tag{2.4}$$

where K_σ is the modified Bessel-function with index σ. Small a expansion of (2.4) at leading order yields

$$V_l(q) \sim g q^\sigma, \text{if} \quad \sigma \neq 0 \tag{2.5}$$

$$V_l(q) \sim g \log(aq), \text{if} \quad \sigma = 0 \tag{2.6}$$

where we used the property $K_{-\sigma}(x) = K_\sigma(x)$ of the Bessel function. The non-universal coefficient coming from the Taylor expansion can be absorbed by the appropriate renormalization of the constant g. Special cases when σ is even gives logarithmic behavior. Effectively it does not change our results. So we focus on the typical term q^σ.

The second quantized version of the action (2.2) can be constructed using standard methods [10, 11]. The generalization of the action to the long-range interacting case is also known [48, 49]. The result is

$$S(\phi_i, \phi_i^\dagger) = \int dt d^d x \{ \sum_i [\phi_i^\dagger \partial_t \phi_i + D_i \nabla \phi_i^\dagger \nabla \phi_i] \} +$$

$$+ \int dt d^d x d^d y \sum_{i<j} \phi_i^\dagger(t,x) \phi_i(t,x) V_{ij}(x-y) \phi_j^\dagger(t,y) \phi_j(t,y) \ . \tag{2.7}$$

The first term describes the evolution of free random walks with diffusion constants D_i. The potential is

$$V_{ij}(x-y) = \lambda_{ij} \delta(x-y) + g_{ij} V(x-y), \tag{2.8}$$

and we refer to λ_{ij}, g_{ij} as short-range and long-range coupling constants respectively.

A dynamic response functional associated with the action (2.7) is

$$Z = \int \mathrm{D}\phi \mathrm{D}\phi^{\dagger} e^{-S(\phi_i, \phi_i^{\dagger})} \tag{2.9}$$

where $\phi_i(x,t)$ is the complex scalar field. After the quantization we may treat $\phi_i^{\dagger}(x,t)$ as the creation operator which creates a particle of sort i at point x at time t. Having the dynamic response functional, correlation functions can be computed as functional averages (path integrals) of monomials of ϕ and $\phi^{\dagger}$ with the weight $\exp\left\{-S(\phi, \phi^{\dagger})\right\}$.

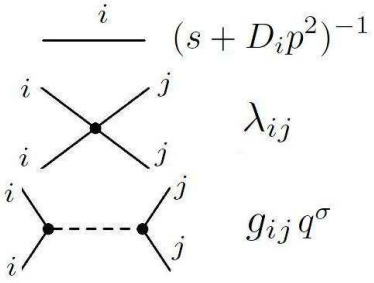

Figure 2.1: Feynman rules for the theory (2.7). Notice that both λ and g vertices appear with different i and j indices and that g has momentum dependence.

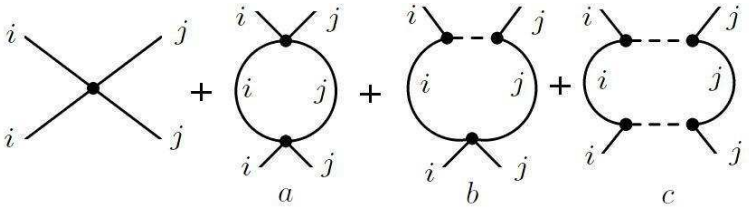

Figure 2.2: One-loop Feynman diagrams contributing to λ_{Rij}.

As a first step towards the renormalization group analysis of this model, we discuss the dimensions of various quantities in (2.7) expressed in terms of momentum:

$$[t] = p^{-2} \quad [\phi] = p^{d} \quad [\lambda] = p^{2-d} \quad [g] = p^{2-d-\sigma}. \tag{2.10}$$

The naive dimension of the coupling constant g allows us to identify the upper critical

dimension $d_c(\sigma) = 2 - d - \sigma$. For $\sigma > 0$, the short-range term naively dominates the long-range term and we expect to have the behavior of the system similar to the case of pure VW. We will reserve the symbol ε ($\varepsilon = 2 - d$) to denote deviations from the short-range critical dimension $d_c = 2$, and δ ($\delta = 2 - d - \sigma$) for the deviations from the long-range critical dimension $d_c(\sigma)$. If $\sigma = 0$ then the critical dimension of the long-range part coincides with the short-range part and we have the non-trivial correction to the asymptotic behavior due to long-range interactions. This boundary separates mean-field or Gaussian behavior from long-range behavior. For $\sigma < 0$ the long-range term dominates the short-range term and we expect to have non-trivial corrections to the behavior of the system.

Now we consider diagrammatic representation elements of model (2.7). In zero-loop approximation the vertex 4-point function takes a simpler form after Laplace-Fourier transformation:

$$\Gamma^{(2,2)}_{ij}(s,p) = V_{ij}(p_1 + p_2)\delta(\sum_k p_k). \tag{2.11}$$

The same transformation applied to the bare propagator yields:

$$\Gamma^{(1,1)}_{j}(s,p) = (s + D_i p^2)^{-1} \tag{2.12}$$

We note that there are no vertices in (2.7) that produce diagrams which dress the propagator, implying there is no field renormalization. As a consequence the bare propagator (2.12) is the full propagator for the theory. Feynman rules are summarized in Figure 2.1. There are two vertices in the theory: one is a short-range λ-vertex and another is a long-range momentum dependent g-vertex. Each external line of the vertex corresponds to a functionally independent field. The propagator is formed by contracting appropriate lines from different vertices. We recall the propagator is the correlation function of ϕ_i and $\phi_i^\dagger$ fields only.

Physical observables are computed with the help of correlation functions. The probability that p sets of particles with n_i particles in each set start at the proximity of the origin and finish at x_{i,α_i} (i index enumerates different sets and α_i index enumerates particles in set i) without intersecting each other can be obtained by generalizing eqn (2.3). In the field theoretical formulation, this probability becomes the following correlation function:

$$G(t) = \int \prod_{i=1}^{p} \prod_{\alpha_i=1}^{n_i} d^d x_{i,\alpha_i} \langle \phi_i(t, x_{i,\alpha_i})(\phi_i^\dagger(0,0))^{n_i} \rangle, \tag{2.13}$$

In the Feynman representation it is the vertex with $2N$ ($N = \sum_j n_j$) external lines. In the first order of the perturbation theory one needs to contract these lines with corresponding lines of the vertices in Figure 2.1. Since there are many independent fields in the correlation function (2.13) this operation can be done in many ways. It yields a combinatorial factor, $n_i n_j$, in front of each diagram, which is the number of ways of constructing a loop from the n_i lines of type i and n_j lines of type j on the one hand and one line of type i and one line of type j on the other hand. From the next section we will see that the survival probability scales as $G(t) \sim t^{-\gamma}$, where γ is the critical exponent. If all walks are free, $\gamma = 0$. In the presence of interactions we expect γ to be a universal quantity that does not depend on the intensity of the short-range interaction λ_{ij}. It is convenient to introduce the so called truncated correlation function which is obtained from (2.13) by factoring out external lines:

$$\Gamma(t) = G(t)/(\Gamma^{(1,1)})^{2N} \tag{2.14}$$

Another physical observable, the reunion probability, is defined as the probability that p sets of particles with n_i particles in each set start at the proximity of the origin and without colliding into each other finish at the proximity of some point

at time t:

$$R(t) = \int d^d x \prod_{i=1}^{p} \langle \phi_i(t,x)^{n_i} (\phi_i^\dagger(0,0))^{n_i} \rangle, \tag{2.15}$$

In the Feynman representation it is depicted as the watermelon diagram with $2N$ stripes. We note that if the theory is free this expression is the product of free propagators and at the large-time limit the return probability scales as $R_{\mathcal{O}}(t) \sim t^{-(N-1)d/2}$. If interactions are taken into account it becomes $R(t) \sim t^{-(N-1)d/2-2\gamma}$, where γ is survival probability exponent. The reason that it enters with the factor 2 is the following. If we cut a watermelon diagram of the reunion probability correlation function in the middle then it produces two vertex diagrams with $2N$ external lines of the survival probability correlation function. As a result the reunion probability is the product of two survival probabilities. It remains true in all orders of perturbation theory. For a rigorous proof we refer to [38].

2.3 The Renormalization of observables

While computing correlation functions like (2.13) perturbatively one faces divergent integrals when $d = d_c$. The convenient scheme developed for dealing with these divergences follows Callan-Symanzik renormalization-group analysis [25, 24]. Within this scheme we start with the bare correlation function $G(t; \lambda, g)$, where $\lambda = \{\lambda_{ij}\}$, and $g = \{g_{ij}\}$ denote the set of bare short-range and long-range coupling constants. In the renormalized theory it becomes $G_R(t; \lambda_R, g_R, \mu)$. From dimensional analysis it follows that

$$G_R(t; \lambda_R, g_R, \mu) = G_R(t\mu; \lambda_R, g_R), \tag{2.16}$$

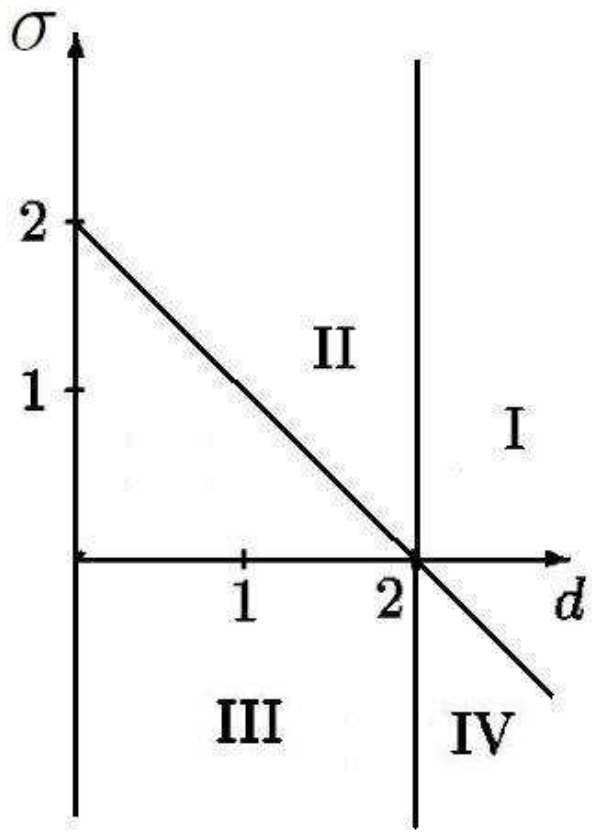

Figure 2.3: The critical behavior of vicious walks with long-range interactions in the different regions of the (σ, d) plane. Region I and IV correspond to the mean field short-range behavior, in region II will be critical short-range behavior, region III is the long-range behavior. The lines $d = 2$ and $\sigma + d = 2$ represent regions V and VI respectively.

where μ is the renormalization scale. The scale invariance leads to the expression

$$G_R(t; \lambda_R, g_R, \mu) = Z(\lambda_R, g_R, \mu) G(t; \lambda, g). \tag{2.17}$$

Here functions Z are chosen in such a way that $G_R(t, \lambda_R, g_R, l)$ remains finite when the cut-off is removed at each order in a series expansion of λ_R, g_R, ε and δ. From the fact that $G(t, \lambda, g)$ does not depend on the renormalization scale μ we get the

Callan-Symanzik equation

$$\left(\mu\frac{\partial}{\partial\mu}+\beta_g\frac{\partial}{\partial g}+\beta_u\frac{\partial}{\partial u}-\gamma\right)G_R=0, \tag{2.18}$$

where the β-functions are defined by

$$\beta_\lambda(\lambda_R,g_R)=\mu\frac{\partial}{\partial\mu}\lambda_R \qquad \beta_g(\lambda_R,g_R)=\mu\frac{\partial}{\partial\mu}g_R \tag{2.19}$$

and the function γ by

$$\gamma(\lambda_R,g_R)=\mu\frac{\partial}{\partial\mu}\ln Z. \tag{2.20}$$

The renormalization group functions are understood as the expansion in double series of coupling constants λ and g and deviations from the critical dimension ε and δ. We take $\delta=O(\varepsilon)$. The coefficient $Z(\lambda_R,g_R,\mu)$ is fixed by the normalization conditions. It is more convenient to impose these conditions on the Laplace transform of the truncated correlation function (2.14). One sets the following condition then

$$\Gamma_R(\mu)=1, \tag{2.21}$$

when $s=\mu$. We note that the same multiplicative renormalization factor Z yields Γ finite. From this fact one can infer that

$$\Gamma(\mu;\lambda,g)=Z(\mu;\lambda,g)^{-1}. \tag{2.22}$$

If we express unrenormalized couplings in terms of renormalized ones (2.22) we will obtain the equation for finding Z explicitly.

The equation (2.18) can be solved by the method of characteristics. Within this method we let couplings depend on the scale which is parametrized by $\mu(x)=x\mu$. Here x is introduced as a parametrization variable of the RG flow and is not to be confused with position. Henceforth x will refer to this parametrization variable. We

introduce running couplings $\bar{\lambda}(x)$ and $\bar{g}(x)$. They satisfy the equations

$$x\frac{d}{dx}\bar{g}(x) = \beta_g(\bar{\lambda}(x), \bar{g}(x)) \quad x\frac{d}{dx}\bar{\lambda}(x) = \beta_\lambda(\bar{\lambda}(x), \bar{g}(x)). \tag{2.23}$$

The renormalized value should be defined by the initial conditions $\bar{\lambda}(1) = \lambda_R$ and $\bar{g}(1) = g_R$. the solution of the equation is then

$$G_R(t) = e^{\int_1^{\mu t} \gamma(\bar{\lambda}(x),\bar{g}(x))dx/x} G_R(\mu^{-1}; \bar{\lambda}(\mu t), \bar{g}(\mu t), \mu) \tag{2.24}$$

Next we calculate the first-order contribution to the renormalized vertices. The λ-vertex is renormalized by the set of diagrams that are shown in Figure 2.2. We notice that there are no diagrams producing the momentum dependent g-vertex in the theory (2.7). This statement is the corollary of the fact that only independent fields of power one enter into the expression of the vertex and there are no higher powers of fields. Also we keep in mind that the renormalized couplings are defined by the value of the vertex function taken at zero external momenta. It produces the following expression:

$$\lambda_{Rij} = \lambda_{ij} - \frac{1}{2}(\lambda_{ij}^2 I_1 + 2\lambda_{ij} g_{ij} I_2 + g_{ij}^2 I_3) \tag{2.25}$$

$$g_{Rij} = g_{ij} \tag{2.26}$$

where $I_k = I_k(\sigma; D_i, D_j)$ are one-loop integrals corresponding to the diagrams a, b, c in the Figure 2.2 respectively. Using the Feynman rules we can explicitly write them down:

$$I_k = \int \frac{d^d q}{(2\pi)^d} \frac{q^{(k-1)\sigma}}{2s + (D_i + D_j)q^2}, \quad k = 1, 2, 3. \tag{2.27}$$

We will use dimensional regularization procedure to compute these integrals. The details of the computation are summarized in Appendix A. We note that integrals

will diverge logarithmically at different values of the spatial dimension d. For this reason it leads to different critical behavior in different regions of the $\sigma - d$ plane (see Figure 2.3). These regions correspond to four possibilities for $\varepsilon = 2 - d$ and $\delta = 2 - d - \sigma$ to be positive or negative. Only if $\delta = O(\varepsilon)$ or, in other words, if both ε and δ are infinitesimally small but the ratio ε/δ is finite we expect non-zero fixed points of the renormalization group flow. Similar approximation have been used before [40] but for different models with long-range disorder. It allows us to follow the standard procedure of deriving the β-functions which consists of two steps.

First, we express unrenormalized couplings in terms of the renormalized. For the short-range coupling constant λ it can be done by solving the quadratic equation in (2.25). Expanding the square root and keeping terms up to the second order we infer that

$$\lambda_{ij} = \lambda_{Rij} + \frac{1}{2}(\lambda_{Rij}^2 \frac{a_d}{\varepsilon} + 2\lambda_{Rij} g_{Rij} \frac{b_d}{\delta} + g_{Rij}^2 \frac{c_d}{2\delta - \varepsilon}) \tag{2.28}$$

$$g_{ij} = g_{Rij} \tag{2.29}$$

where a_d, b_d and $c_d$coefficients have been found explicitly in Appendix A. Now we introduce dimensionless renormalized couplings

$$\bar{g}_{Rij} = a_d (2s)^{-\delta/2} \quad \bar{\lambda}_{Rij} = b_d (2s)^{-\varepsilon/2}. \tag{2.30}$$

An important observation is that $c_d a_d = b_d^2$ which can be verified by explicit substitution (see Appendix A). Multiplying the first and second equation in (2.28) by the factors a_d and b_d respectively, and using redefinitions (2.30) we can condense all pre-factors in the right hand side of the equations into the dimensionless constants.

Second, we differentiate equations (2.28) with respect to the scaling parameter μ. Using definitions (2.19) and the fact that bare couplings do not depend on

the scale, we derive

$$\beta_{\lambda,ij} = -\varepsilon\bar{\lambda}_{Rij} + (\bar{\lambda}_{Rij} + \bar{g}_{Rij})^2 \tag{2.31}$$

$$\beta_{g,ij} = -\delta\bar{g}_{Rij} \tag{2.32}$$

where the right hand side is understood as the leading contribution to the β-functions from the double expansions in λ, g and ε, δ. From (2.31) we see that it is convenient to introduce new coupling constants $u_{Rij} = \bar{\lambda}_{Rij} + \bar{g}_{Rij}$. After this step the renormalization group equations read

$$\beta_{u,ij} = -\varepsilon u_{Rij} + u_{Rij}^2 - g_{Rij} \tag{2.33}$$

$$\beta_{g,ij} = -\delta g_{Rij} \tag{2.34}$$

We note that in the last equations g coupling constant has been redefined $\sigma\bar{g}_{Rij} \to g_{Rij}$.

Fixed points are zeros of the β-functions. If $\delta \neq 0$ then the last equation in (2.33) is zero only when $g_* = 0$. Then the first equation has two solutions $u = 0$ and $u = \varepsilon$. If $\delta = 0$ then g plays the role of a parameter and the fixed points are determined by the roots of the quadratic equation

$$0 = -\varepsilon u + u^2 - g \tag{2.35}$$

which are real if $g \geq -(\varepsilon/2)^2$ and we find

$$u_{1,2} = \varepsilon/2 \pm \sqrt{(\varepsilon/2)^2 + g}. \tag{2.36}$$

All fixed points are listed in the Table 2.2. The stability of these fixed points is

determined by the matrix of partial derivatives

$$\beta_* = -\left(\begin{array}{cc} \partial\beta_u/\partial u & \partial\beta_u/\partial g \\ \partial\beta_g/\partial u & \partial\beta_g/\partial g \end{array} \right)_{u=u_*, g=g_*} \tag{2.37}$$

Eigenvalues are listed in the Table 2.2. The Gaussian fixed point is stable in all directions for $\varepsilon < 0$ and $\delta < 0$ which corresponds to region I in Figure 2.3. In this region we find both short-range(pure VW) and long-range mean-field behavior depending on the sign of σ.

On the contrary, for $\varepsilon > 0$ and $\delta > 0$ we find that the Gaussian fixed point is unstable(irrelevant) in all directions and the short-range (pure VW) fixed point is stable(relevant) only in u-direction. It means that long-range interactions will play a leading role. This region corresponds to region III in Figure 2.3. Next for $\varepsilon > 0$ and $\delta < 0$ we find that the short-range (pure VW) fixed point is stable in all directions. It means that the system is insensitive to the long-range tail. This region corresponds to region II in Figure 2.3. Finally for $\varepsilon < 0$ and $\delta > 0$ we find that the short-range (pure VW) fixed point is unstable in all directions and the system will be described by mean-field at long time.

2.4 Calculation of critical exponents and discussion

Here we describe our method of computing critical exponents. It is based on the formula (2.22) from the previous section. First, we obtain the leading divergent part of the correlation function. The renormalized correlation function depends on the scale μ but it appears in all formulas in combination with time: μt. Second, since we have found the bare coupling constant as a function of renormalized (dressed) couplings we express correlation function in terms of dressed couplings. Finally

Table 2.2: Fixed points for flow equations (2.33) and the corresponding eigenvalues (λ_1, λ_2) of the stability matrix (2.37). We note that u_1 and u_2 are defined by equation (2.36). LR stands for long-range.

Fixed point	(u_*, g_*)	(λ_1, λ_2)
Gaussian	$(0, 0)$	(ε, δ)
Pure VW	$(\varepsilon, 0)$	$(-\varepsilon, \delta)$
LR stable	$(u_1, 0)$	$(-\sqrt{\varepsilon^2 - 4g}, 0)$
LR unstable	$(u_2, 0)$	$(\sqrt{\varepsilon^2 - 4g}, 0)$

using the normalization condition (2.21) and the definition (2.20) we differentiate Z with respect to $\mu\partial/\partial\mu$ to obtain the exponent γ. The poles should cancel after this operation.

In section 2 it was explained that the truncated correlation function in the one-loop approximation is given by the formula

$$\Gamma(t; \lambda, g) = 1 - \sum_{i,j} n_i n_j \left(\lambda_{ij} I_1 + g_{ij} I_2\right). \tag{2.38}$$

Here integrals are the same as in (2.27).

We start our analysis with the region I. Notice that truncated correlation function $\Gamma(t)$ and survival probability $G(t)$ have similar large time behavior. We use large momentum cut-off to compute integrals I_1 and I_2 as in formula (5.9) in Appendix A. The renormalization of coupling constants is trivial in this case. Therefore the leading contribution to the survival probability is given by

$$G(t) \sim t^{(2-d)/2} + g_0 t^{(2-d-\sigma)/2}, \tag{2.39}$$

where g_0 is non-universal coefficient and we will not need its exact value. We notice

that if $\sigma > 0$ the second term will decay faster than the first term and in the long-time limit it will produce the same behavior as mean-field pure VW. On the other hand if $\sigma < 0$ the first term will decay faster and long-range interactions will play a leading role. Many authors observed similar behavior in various systems with long-range defects [40, 41, 42]. Intuitively if potential falls fast with distance than the system effectively represent system with short-range potential where particle interact when they are close to each other.

Region IV exhibits similar behavior. Now the integral I_2 is computed with the help of the dimensional regularization (5.3) and the integral I_1 remains the same. From the fact (2.16) one can infer that the survival probability scales as

$$G(t) \sim t^{(2-d)/2}. \tag{2.40}$$

Short-range behavior dominates because the running coupling constant will flow towards the Gaussian fixed point at long time limit which is the only stable fixed in this region. This result is exact regardless the number of loops one takes into account.

In Region II the computation is as follows.

$$\ln Z = \sum n_i n_j \left(\lambda_{ij} \frac{a_d}{\varepsilon} + g_{ij} t^{(2-d-\sigma)/2} \right), \tag{2.41}$$

so plugging the result from (5.4) to (2.41) we obtain at the fixed point ($\lambda_* = \varepsilon, g = 0$)

$$\gamma = -\frac{1}{2} \sum n_i n_j \varepsilon \tag{2.42}$$

And we reproduce the pure VW behavior. This result is the reflection of the fact that the renormalization-group trajectories run away to stable pure VW fixed point. It is with agreement with the results obtained by Katori in [46] for $d = 1$, and the logarithmic intraset particle interactions. The irrelevance of the long-range interaction

in lower dimensions is a typical phenomenon observed in a various out of equilibrium interacting particle systems.

We now consider regions III, V and VI. Integrals in (2.38) are computed via dimensional regularization. Taking the inverse of (2.38) and then logarithm one can obtain at the leading order:

$$\ln Z = \sum n_i n_j \left(\lambda_{ij} \frac{a_d}{\varepsilon} + g_{ij} \frac{b_d}{\delta} \right) \tag{2.43}$$

where a_d and b_d are defined in Appendix A in (5.4) and (5.5). We note that after taking the derivative the poles in (2.43) will cancel in the limit of $\delta = O(\varepsilon)$. Also one recalls the expansion (2.28) and the redefinitions in (2.30). Using (2.20) we show that the expression for the function γ which determines critical exponent takes the form

$$\gamma = -\frac{1}{2} \sum_{ij} n_i n_j u_R \tag{2.44}$$

Evaluated at the stable fixed point ($u_1 = \varepsilon/2 + \sqrt{(\varepsilon/2)^2 + g}$ it gives the following result:

$$\gamma = -\frac{1}{2} \sum_{ij} n_i n_j u_1, \tag{2.45}$$

and the survival probability scales as $G(t) \sim t^{\gamma}$.

We will now find the logarithmic corrections to this scaling law. The running coupling constant can be found from the flow equation (2.33): $\bar{g}(x) = e^{-\delta x} g$. In the case $\delta, \varepsilon = 0$ (the intersection of regions V and VI) the flow equation for $\bar{u}(x)$ is

$$x \frac{d\bar{u}(x)}{dx} = -\bar{u}^2(x) + g \tag{2.46}$$

and the solution is

$$\bar{u}(x) = \sqrt{g}\tanh(\sqrt{g}\ln x + \phi_0) \sim \sqrt{g}\tanh(\sqrt{g}\ln x), \tag{2.47}$$

where ϕ_0 is the initial condition and we do not need its exact form. After plugging this expression into the (2.24) we infer

$$\int_1^{\mu t} \gamma(\bar{u}, \bar{g})\frac{dx}{x} \sim \ln(\cosh(\sqrt{g}\ln \mu t)) \tag{2.48}$$

Thus the survival probability is

$$G(t) \sim \cosh(\sqrt{g}\ln t)^{-\frac{1}{2}\sum n_i n_j} \tag{2.49}$$

In the limit of large time $\cosh(\sqrt{g}\ln t) \sim t^{\sqrt{g}}$ implying $gamma = -\frac{1}{2}\sum_{ij} n_i n_j \sqrt{g}$ which is consistent with equation (2.45). For negative coupling constant $g < 0$ the solution in (2.47) becomes

$$\bar{u}(x) \sim -\sqrt{|g|}\tan(\sqrt{|g|}\ln x) \tag{2.50}$$

The integral (2.48) is divergent if $t > \exp(\pi/2\sqrt{|g|})$ which leads to the result that the survival probability is zero beyond this time. For smaller times one has $G(t) \sim \cos(\sqrt{|g|}\log t)^{-\frac{1}{2}\sum n_i n_j}$. Thus, upto one-loop order approximation, It implies that if walks are attracted to each other then all of them will annihilate at some finite time. This might be a signature of faster than power law decay and we expect to have corrections to this behavior at higher loop approximation.

Next we consider the case when $\varepsilon = 0$ and $\delta \neq 0$ but δ remains small i.e. region V. The flow equation for the $\bar{u}(x)$ is

$$x\frac{d\bar{u}(x)}{dx} = -\bar{u}^2(x) + gx^{-\delta} \tag{2.51}$$

and the solution can be found by the method of perturbation. Up to the first order

$$\bar{u}(x) = \sqrt{g}\tanh(\sqrt{g}\ln x) + \delta\sqrt{g}\ln(x)\tanh(\sqrt{g}\ln x) \tag{2.52}$$

After plugging this expression into eqn (2.24) we infer

$$\int_1^{\mu t} \gamma(\bar{u},\bar{g})\frac{dx}{x} \sim -\frac{1}{2}\sum n_i n_j \left(\ln(t^{\sqrt{g}}) + \frac{1}{2}\delta\sqrt{g}\ln^2(t)\right) \tag{2.53}$$

Therefore we have the correction to the survival probability in the form

$$G \sim t^{-\frac{1}{2}\sum n_i n_j \sqrt{g}(1+\delta/2(\ln t))} \tag{2.54}$$

Now we extend our analysis to the case when $\varepsilon > 0$, corresponding to regions III and VI. The evolution of the coupling constant is

$$x\frac{d}{dx}\bar{u}(x) = \varepsilon\bar{u} - \bar{u}^2 + gx^{\delta} \tag{2.55}$$

We choose the ansatz in the form $\bar{u}(x) = u_0(x) + \delta v(x)$. For $\delta = 0$ (i.e. region VI) the equation for $u_0(x)$ reads

$$x\frac{d}{dx}u_0(x) = \varepsilon u_0 - u_0^2 + g \tag{2.56}$$

and we reproduce the result (2.45). We now extend to the case where $\varepsilon, \delta > 0$ (region III). Here we will need the exact solution to (2.56) to find the corrections:

$$u_0(x) = \frac{Cx^{u_1-u_2}u_1 + u_2}{1 + Cx^{u_1-u_2}}, \tag{2.57}$$

where $C = (u_R - u_2)/(u_1 - u_R)$. The logarithmic correction follows from the form of the perturbation. The equation for $v(x)$ is

$$x\frac{d}{dx}v(x) = \varepsilon v - 2u_0 v - g\ln x \tag{2.58}$$

The solution can be found explicitly as a combination of hypergeometric functions. In

the most interesting case, $\varepsilon = 1$ ($d = 1$) the hypergeometric functions are degenerate and become linear functions. Corrections to the integral then read

$$\int_1^{\mu t} \gamma dx/x \sim \frac{1}{2}\delta u_1 \ln^2(t) + \ln(t)(t)^{u_1 - u_2}) \tag{2.59}$$

In the limit of large time only the first term contributes to the exponent and the survival probability scales as

$$G \sim t^{-\frac{1}{2}\sum n_i n_j u_1 (1+\delta/2 \ln t)} \tag{2.60}$$

Chapter 3

Vicious Lévy flights

3.1 Introduction

Diffusive processes with long range jumps play an important role in many physical, chemical and biological phenomena. A Lévy flight is an example of such a process where the probability distribution of the length of an individual step, r, is governed by the power-law $r^{-d-\sigma}$, where d is the dimension of the space and σ is the Lévy exponent. Smaller values of σ therefore produce longer range jumps while for $\sigma \geq 2$, the mean jump length is finite and simple diffusive behavior is recovered. Lévy flights have been used to describe a wide range of processes including epidemic spreading, transcription factor proteins binding to DNA, kinetic Ising models with long-range interactions, foraging animals and light propagation in disordered optical materials [51, 52, 53, 54, 8, 55, 56, 57, 58]. While individual Lévy flights have been studied in great detail, the same is not true if we consider several distinct groups of Lévy flights. One could, for example, be interested in the statistics of encounters between members of different groups. This question is relevant for processes where the outcome depends on the occurrence of such encounters. Examples include sharks and other marine animals searching for prey [22], chemical reactions in turbulent environments [51], electron-hole recombination in disordered media [59] and even male spider-monkeys encountering their mates or other aggressive males in the forest

[23].

In this chapter we compute the survival probability, i.e. the probability that no two members of different groups of Lévy flights have met up to time t. For the case of simple diffusion with exactly one particle in each group, this corresponds to the classic problem of Gaussian vicious walks [14], i.e. walks that are prohibited from being on the same site at the same time, but remain independent otherwise. Here we generalize this concept to groups of Lévy flights under the same constraints. We term them vicious Lévy flights (VLF). We consider p sets of particles with n_i particles in each set, $i = 1 \dots p$, that are driven by Lévy noise on the d dimensional regular lattice. A pairwise interset short-range (delta-function) interaction is introduced to guarantee that trajectories which continue beyond an intersection are discarded, i.e. have zero statistical weight. This terminates the process at the first encounter between members of different groups. Particles belonging to the same set do not interact. We note that Lévy flights are allowed to jump over each other, unlike ordinary random walks which can only jump to neighboring sites and can not intersect with the vicious constraint. In $d = 1$ this means that the ordering is preserved for vicious walks but not for VLF. For simplicity we assume that Lévy exponents for all flights are the same. Generalization to the case of different Lévy exponents will be done elsewhere. At time $t = 0$ all particles start in the vicinity of the origin. We are interested in the survival probability of this system at late times.

3.2 RG flow equations and fixed points

We start with a field theoretic formulation of the problem. Methods to formulate field theories for such stochastic systems are well established [10, 11]. Specifically for Gaussian vicious walks, such a formulation exists [15] and the form of the action is known. We can adapt the action to our case by replacing the Laplacian

∇^2 with the operator ∇^σ that generates long-range jumps. This gives

$$S(\phi_i, \phi_i^\dagger) = \int dt d^d x \sum_{i=1}^{p} [\phi_i^\dagger \partial_t \phi_i + \phi_i^\dagger \nabla^\sigma \phi_i] +$$

$$+ \sum_{1 \le i < j \le p} \lambda_{ij} \phi_i^\dagger(t,x) \phi_i(t,x) \phi_j^\dagger(t,x) \phi_j(t,x), \tag{3.1}$$

where $\phi_i(x,t)$ are p complex order parameters corresponding to p different sets of equivalent Lévy flights and λ_{ij} are coupling constants corresponding to interset interactions. The non-intersection property of VLF arises from the choice $\lambda_{ij} \to \infty$ but we will show that to leading order the survival probability does not depend on the particular value of these coupling constants. This action is also similar to the action for the reaction-diffusion problem with long-range interactions [60, 61]. Power counting shows that the upper critical dimension for the above field theory is $d_c = \sigma$ for $\sigma < 2$ and $d_c = 2$ for $\sigma \ge 2$. VLF exhibit different phases (see inset Figure 3.1) depending on the values of d and σ. In the mean field phase for $d > d_c$ (Region I), the survival probability of VLF is non-zero at infinite time because the walks become non-recurrent and particles can avoid each other for all time. For $\sigma \ge 2$ (Region II) VLF reproduce Gaussian vicious walks. For $d < \sigma < 2$ (Region III) we expect fluctuations to play an important role. In this phase, we will obtain the critical behavior of the survival probability using ε-expansion ($\varepsilon = \sigma - d$) around mean field theory in two-loop approximation.

We now turn to the renormalization group analysis. The propagator given by (3.1) is

$$\Gamma_j^{(1,1)}(s,k) = (s + k^\sigma)^{-1}. \tag{3.2}$$

The particular form of the vertex in (3.1) leads to the fact that there are no diagrams which dress the propagator. This implies that the bare propagator is the exact

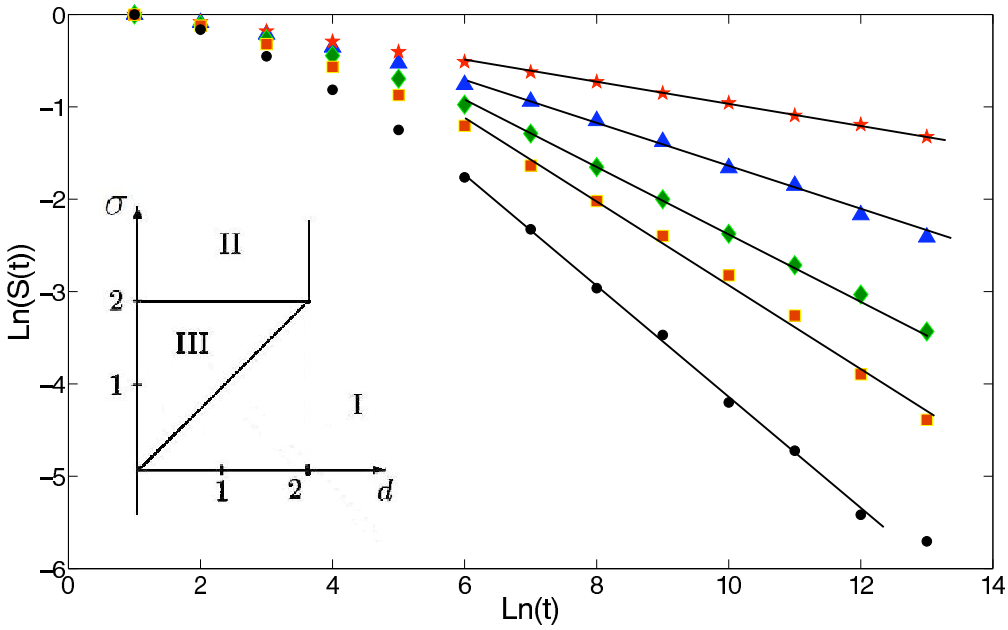

Figure 3.1: a. $\ln(S)$ vs $\ln(t)$ for two identical VLF in $d = 1$. σ values from top tp bottom are $1.1, 1.3, 1.5, 1.7, 2.5$ respectively. Symbols represent simulation data and solid lines correspond to best fit lines to the late time data. Inset: Domains of VLF exponents in the $\sigma - d$ plane.

propagator for the theory. The proper vertex is defined by factoring out external legs from the ordinary 4-point Green's function of (3.1) $G^{(2,2)}_{ij}(s_l, k_l; \lambda)$. Here $\lambda = \{\lambda_{ij}\}$ is the collection of coupling constants and (s_l, k_l) for $l = 1 \ldots 4$ are the energy (Laplace image of time) and momenta respectively [62]. This yields

$$\Gamma^{(2,2)}_{ij}(s_l, k_l; \lambda) = \frac{G^{(2,2)}_{ij}(s_l, k_l; \lambda)}{\prod_{m=1}^{4} \Gamma^{(1,1)}(s_m, k_m)}. \tag{3.3}$$

The renormalized coupling, λ_{Rij}, is the value of the proper vertex at $(s_l = \mu, k_l = 0)$, for all l, where μ is a renormalization group flow scaling parameter. It is possible to

sum all diagrams in the series with the result

$$\lambda_{Rij} = \lambda_{ij}(1 + \lambda_{ij} I_1)^{-1}, \tag{3.4}$$

where

$$I_1 = (2\pi)^{-d} \int d^d q (2\mu + 2q^\sigma)^{-1}. \tag{3.5}$$

The value of the integral I_1 is given by $I_1 = A\mu^{-\varepsilon/\sigma}\varepsilon^{-1}$, where

$$A = \frac{\varepsilon\Gamma(d/\sigma)\Gamma(\varepsilon/\sigma)}{2^d \pi^{d/2}\sigma\Gamma(d/2)} = \frac{2^{-\sigma}\pi^{-\sigma/2}}{\Gamma(\sigma/2)} + O(\varepsilon), \tag{3.6}$$

is the geometric factor at the leading order in $\varepsilon = \sigma - d$. By introducing the redefined coupling constant

$$g_{Rij} = \lambda_{Rij}\mu^{-\varepsilon/\sigma}, \tag{3.7}$$

we obtain the following renormalization group flow equations (see Appendix B for details):

$$\mu \frac{\partial g_{Rij}}{\partial \mu} = (-\varepsilon + A g_{Rij}) g_{Rij}/\sigma. \tag{3.8}$$

The fixed point of this flow is

$$g_* = \varepsilon A^{-1}. \tag{3.9}$$

We note that this value of the fixed point is exact to all orders since all diagrams were taking into account in (3.4). The stability of the fixed point follows from the fact that

$$-\partial\beta_{ij}/\partial g_{Rij}|_{g_{Rij}=\varepsilon/A} = -\varepsilon/\sigma < 0 \tag{3.10}$$

in the VLF region, where $\beta_{ij} = \mu\partial g_{Rij}/\partial\mu$ is renormalization group beta function.

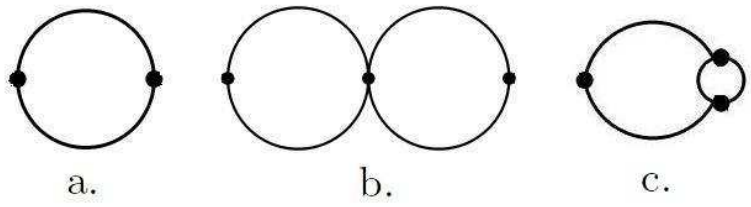

Figure 3.2: a. 1-loop diagram corresponding to the integral I_1 b., c. 2-loop intgrals corresponding to I_1^2 and I_2 respectively.

3.3 Survival probability exponent computation

We now consider the survival probability which is defined as the correlation function [15]

$$S(t;\lambda) = \int \prod_{i=1}^{p} \prod_{\alpha_i=1}^{n_i} d^d x_{i,\alpha_i} \langle \phi_i(t, x_{i,\alpha_i})(\phi_i^\dagger(0,0))^{n_i} \rangle, \tag{3.11}$$

with the measure $\int \mathcal{D}\phi^\dagger \mathcal{D}\phi \exp[-\mathcal{S}]$. The Feynman diagram of (3.11) at zero order is a vertex with $2N$ external legs. Similar to the case of the $(2,2)$-vertex it is convenient to work with the truncated correlation function

$$\Gamma(s_l, k_l; \lambda) = S(s_l, k_l; \lambda) / \prod_{m=1}^{2N} \Gamma^{(1,1)}(s_m, k_m). \tag{3.12}$$

The finite renormalized truncated correlation function $\Gamma_R(s_l, k_l; \lambda_R, \mu)$, where $\lambda_R = \{\lambda_{Rij}\}$ is a collection of renormalized coupling constants, is related to the bare truncated correlation function by

$$\Gamma_R(s_l, k_l; \lambda_R, \mu) = Z(\lambda, \mu)\Gamma(s_l, k_l; \lambda), \tag{3.13}$$

where $Z(\lambda, \mu)$ is the scaling function. From this one obtains the renormalization group equation for $\Gamma_R(s_l, k_l; \lambda_R, \mu)$ using the chain rule

$$(\mu \frac{\partial}{\partial \mu} + \beta_{ij} \frac{\partial}{\partial g_{Rij}} + \gamma)\Gamma_R(s_l, k_l; \lambda_R, \mu) = 0, \tag{3.14}$$

where $\gamma = \mu\partial \ln Z/\partial\mu$. At the fixed point (3.14) reduces to $(\partial/\partial \ln(\mu)+\gamma_*)\Gamma_R(s,\mu) = 0$ whose solution is

$$\Gamma_R \sim \exp(\int_0^\mu \gamma_* d(\ln(\mu'))), \tag{3.15}$$

where $\gamma_* = \mu\partial \ln Z/\partial\mu|_{g_{Rij}=g_*}$. Since γ_* is constant at the fixed point we have $\Gamma_R \sim \mu^{-\gamma_*}$. The fact that the dimensions of field and the action are $[\phi^\dagger] = [\phi] = k^{d/2}$ and $[\mathcal{S}] = \infty$ implies that $[S] = 1$. Thus it follows that the survival probability can only be a function of the dimensionless product μt. From this one infers that the asymptotic behavior of the survival probability is $S(t) \sim t^{-\gamma_*}$ which gives $\alpha = \gamma_*$. In order to find Z one uses a normalization condition on Γ_R that fixes the value of Z. This can be chosen as $\Gamma_R(s_l, k_l; \lambda_R, \mu) = 1$ when $s_l = \mu$ and $k_l = 0$ for all l. This implies that

$$Z = \Gamma(\mu, 0; \lambda)^{-1}. \tag{3.16}$$

$\Gamma(\mu, 0; \lambda)$ can be expressed as a series, up to two-loop order, of the integrals corresponding to the diagrams shown in Figure 3.2 with appropriate combinatorial factors originating from the number of distinct ways in which propagators can be assigned to the same diagram. I_1 was evaluated before. The integral corresponding to the diagram 2c is

$$I_2 = \int \frac{d^d k d^d q}{(2\mu + 2k^\sigma)(3\mu + q^\sigma + k^\sigma + |k+q|^\sigma)} \tag{3.17}$$

This can be evaluated using Mellin-Barnes representation [63] which replaces the sum in the denominator of $|k+q|^\sigma$ and q^σ by the product of these terms raised to some power. The result for I_2 up to the leading order reads

$$I_2 = \frac{2^{-2\sigma}\pi^{-\sigma}}{\Gamma(\sigma/2)^2}\mu^{-2\varepsilon/\sigma}\left(\frac{1}{2\varepsilon^2} + \frac{2(-\ln(3/4)/4 + C)}{\sigma\varepsilon}\right), \tag{3.18}$$

where

$$C = [\psi^{(0)}(\sigma/2) + \ln(4\pi)]/2 \tag{3.19}$$

and $\psi^{(0)}(x)$ is standard digamma function. The details of the calculations are summarized in Appendix C. Knowing I_1, I_2 and the appropriate combinatorial factors allows us to evaluate $\Gamma(\mu, 0; \lambda)$ and therefore $Z(\mu, \lambda)$ as a series. Differentiating $\ln Z$ with respect to μ and substituting λ with λ_R (inverting (3.4)) and then taking the value at the fixed point gives us the survival probability exponent $\alpha = \gamma_*$, with the final result (see Appendix D):

$$\alpha = \sum_{1 \le i < j \le p} n_i n_j \varepsilon/\sigma + \ln(3/4) Q \varepsilon^2/\sigma^2, \tag{3.20}$$

where

$$Q = 6 \sum_{1 \le i < j < k \le p} n_i n_j n_k + \sum_{1 \le i < j \le p} n_i n_j (n_i + n_j - 2). \tag{3.21}$$

At the critical dimension $d = d_c = \sigma$ we see that the fixed point coincides with the Gaussian point. The interaction becomes marginal in the renormalization group sense. Equation (3.8) then yields the flow equations for the running coupling constant

$$x d\bar{g}_{ij}(x)/dx = A \bar{g}_{ij}^2(x)/\sigma, \tag{3.22}$$

with initial condition $\bar{g}_{ij}(1) = g_{Rij}$. Solving this and substituting the result into (3.15) we get $S(t) = (\ln t)^{-\alpha_l}$, where

$$\alpha_l = \sum_{1 \le i < j \le p} n_i n_j. \tag{3.23}$$

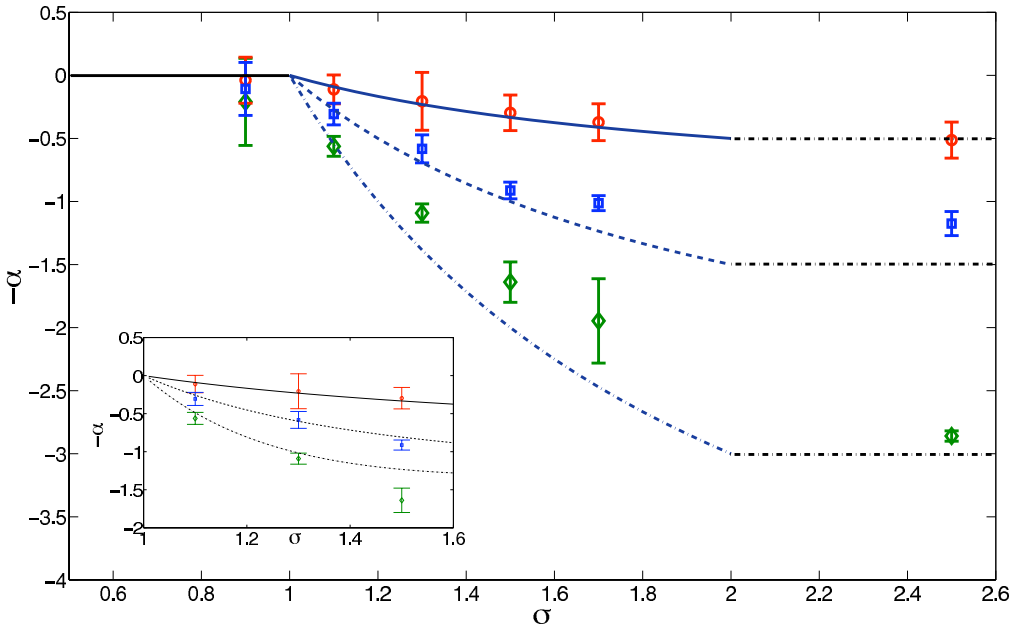

Figure 3.3: α as a function of σ for $d = 1$. Symbols with error bars represent simulation data corresponding from top to bottom to $N = 2, 3, 4$ VLF respectively. Lines correspond to 1-loop approximation from formula (3.20) for $1 < \sigma < 2$. For $\sigma < 1$, $\sigma \geq 2$ lines represent the mean field and Gaussian exponents respectively. Inset: Same simulation data compared to 2-loop approximation from (3.20).

3.4 Comparison with numerical results and discussion

Now we describe the details of the numerical simulation that we used to confirm our results in $d = 1$. At $t = 0$ we start with $N = \sum_{i=1}^{p} n_i$ particles belonging to p distinct sets placed equidistantly on the lattice. At each time step we generate N random variables, x_j, drawn from the uniform distribution on the interval $(0, 1)$. Each particle jumps a distance $l_j = x_j^{-1/\sigma}$ with equal probability to the left or to the right. This procedure generates an independent Lévy flight trajectory for each particle. The process stops whenever particles from different sets land on the same

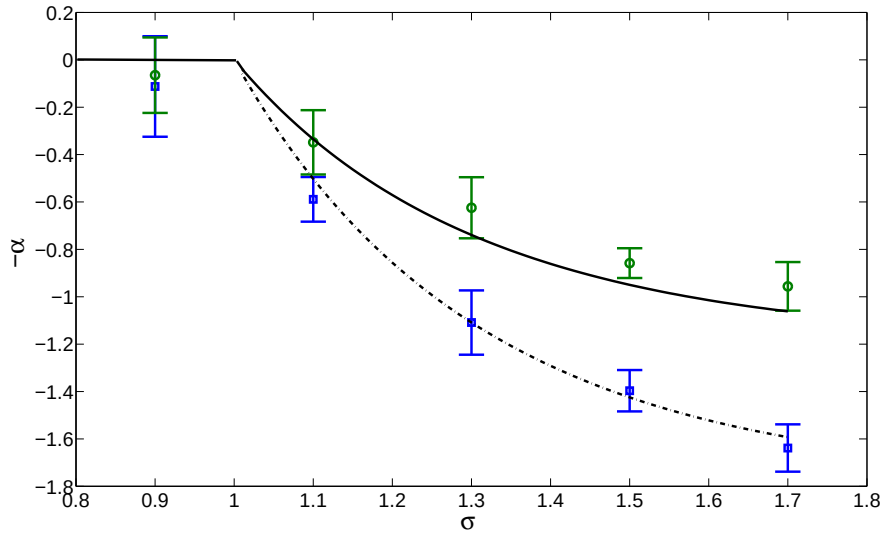

Figure 3.4: α vs σ for predator and prey problem in $d = 1$. Symbols represent simulation data for 4 predators and 1 prey (circles) and 3 predators and 2 prey (squares). Lines are 2-loop approximation from formula (3.20).

site. We perform $\sim 10^5$ iterations for each set of parameter values. The survival probability $S(t)$ is defined by the number of processes that survived beyond time t divided by the total number of iterations. Figure 3.1 shows the plot of the survival probability as a function of time for $N = 2$ for different values of σ. It is clear that at late times $\ln S(t)$ is linear in $\ln t$ verifying our predicted power-law decay $S(t) \sim t^{-\alpha}$. The critical exponent α is evaluated from the slope of the best fit line of the late time data.

We first consider systems with exactly one particle in each set. Figure 3.3 shows the value of exponent α for various values of σ with the total number of particles $N = 2, 3$ and 4 in $d = 1$. Values of $\sigma \geq 2$ will reproduce Gaussian vicious walks and we therefore expect our exponents to approach the exact Fisher exponents [14] as seen in Figure 3.3. For two VLF higher loop corrections are absent (see (3.20)) and the one-loop result is an exact result in agreement with the simulation. It is

interesting to note that the survival probability for the $N = 2$ case is equivalent to the first return probability of a single Lévy flight to the origin after time t which scales as $t^{-1+d/\sigma}$ [64] and matches our results. For $\sigma < 1$, or $d > d_c$, we expect mean field behavior where survival probability at late times approaches a non-zero value implying that there is a finite probability that Lévy flights with $\sigma < 1$ will never find each other. The fact that the survival probability tends to a constant at late times is reflected in the small values of α for $\sigma = 0.9$. For $1 < \sigma < 2$, the mean field behavior is incorrect and we expect the fluctuations to shift the decay exponent to some non-trivial value. For σ close to one, the 1-loop result is in good agreement with the simulation. For larger values of σ, the 2-loop corrections perform better (see Figure 3.3 inset). It is to be noted that the discrepancy between theory and simulation becomes large for higher values of N because the combinatorial factors in (3.20) become large and we therefore need to keep higher order terms in ε for the same degree of accuracy. It is interesting that the 1-loop approximation works reasonably well over the entire range of $1 < \sigma \leq 2$ simply because the 1-loop term in (3.20) happens to give the exact Fisher result if we set $\sigma = 2$. We notice that in all cases the value of the survival probability exponent α increases with σ starting from $\alpha \sim 0$ at $\sigma < 1$ and rising to the value of the Fisher exponents for the equivalent Gaussian vicious walks. This is in contrast to diffusion-annihilation reactions with long-range jumps where the density of reactants decays faster for smaller values of σ [61].

We now consider a system that consists of 2 sets of identical VLF with different numbers of independent particles in each set. We shall call one set predators and the other set prey. Figure 3.4 compares the values of the 2-loop exponents to the simulation results for various values of σ for two different cases: 4 predators - 1 prey and 3 predators - 2 prey. Similar to the previous case we have mean field

and Gaussian behaviors for $\sigma < 1$ and $\sigma \geq 2$ respectively. The Gaussian case is also known as the lion-lamb problem and has been studied before [34]. Unlike the lion-lamb problem, however, our results do not depend on the initial ordering of predators and prey because ordering is not preserved for VLF. For a given σ and total number of predators plus prey, the number of potentially lethal encounters is maximized when the difference between the number of predators and prey is the smallest implying that the survival probability will decay faster as seen in Figure 3.4.

Chapter 4

Conclusions

In this dissertation we studied the statistics of encounters of random walks. In particular, we examined two interesting generalizations of the classic problem of vicious walks introduced by Fisher [14] more than 25 years ago, which has since found innumerable applications. Vicious walks are random walks that are prohibited from being on the same site at the same time, but remain independent otherwise, or in other words, the process is terminated upon the first encounter between independent walkers, leading to the name "vicious walks". An important quantity describing these processes is the survival probability $S(t)$, that the process survives upto time t. We considered the general problem of distinct groups of walks, where members of each group were only vicious to members of other groups, in two different contexts and computed the survival probability in each case.

Our first problem looked at the case where vicious walkers also experienced a long range inter-walker interaction of the form r^{-s-d} . This generalization was motivated by trying to understand the statistics of encounters in a wide range of systems such as metastable supercooled liquids [27], melting in type-II high-temperature superconductors [28], electron transport in quasi-one-dimensional conductors [29] and carbon nanotubes [30], radiolysis in liquids [31], electronic energy transfer reactions [32], interacting predator-prey models [34] and membrane inclusions with curvature-

mediated interactions [16]. We showed that below the critical dimension ($d_c = 2$), the asymptotic form of the survival probability is $S \sim t^{-\alpha}$. We calculated α for all values of s and d to first order in $\varepsilon = 2 - d$ expansion and to all orders in $\delta = 2 - d - s$ expansion, which have hitherto been known only for $d + s = 2$. Our results indicate that, depending on the exact values of d and s, the system can be dominated by either short range (pure VW) or long range behaviors. In addition, we calculated the leading logarithmic corrections for several dynamical observables that are typically measured in simulations. Since our results are very general we are confident that they can be applied to many situations of interest, such as the ones mentioned above. We hope that our work stimulates further interest in long-range vicious walks. It would be interesting to see further simulation results for the critical exponents for $d > 1$ and for logarithmic corrections. Also, it would be interesting to have analytical and numerical results for other universal quantities such as scaling functions and amplitudes.

In the second problem we introduced a novel generalization of the vicious walk problem - vicious Lévy flights (VLF) - independent groups of Levy flights where the process is stopped upon the first encounter between members of different groups. Our motivation was the following. Diffusive processes with long range jumps such as Levy Flights play an important role in many physical, chemical and biological phenomena. Examples include epidemic spreading, transcription factor proteins binding to DNA, kinetic Ising models with long-range interactions, foraging animals and light propagation in disordered optical materials. In many cases, the statistics of encounters between entities performing Levy flights is of significant interest. These encounters can, in fact, affect the outcome of these processes. These include not only traditional condensed matter/physical systems such as chemical reactions in turbulent environments or electron hole recombination in disordered materials but

also biological/ecological processes including encounters between marine predators and prey as well as foraging animals such as albatrosses and spider monkeys. We used renormalization group analyses to compute the late time behavior of the survival probability of this system, which directly translates into understanding the time before the first encounter. We showed that the probability that the process survives up to time t decays as $t^{-\alpha}$ at late times just as in the previous case. We computed α up to the second order in ε-expansion, where $\varepsilon = \sigma - d$, σ is the Lévy exponent and d is the spatial dimension. For $d = \sigma$, we found the exponent of the logarithmic decay exactly. Theoretical values of the exponents were confirmed by numerical simulations. There are several aspects of our work that make it exciting. Firstly, it addresses an unanswered question regarding the statistics of encounters between groups of Levy flights, an interesting statistical mechanical problem in its own right. Secondly, it introduces a completely novel and unstudied process- VLF. Thirdly, we computed upto two loop order, the critical exponents for this new class of processes for the first time and furthermore we performed careful numerical simulations to validate the values of these new exponents. Finally, the methods we have developed should be helpful to study other field theoretic actions with fractional derivatives. An interesting extension would be to solve the problem in the general case of particles with different diffusion constants and Lévy exponents. The predictive power of the ε-expansion for VLF, that we have demonstrated, should be useful in many applications of practical importance. Examples include the optimization of the predator-prey search [65] or trapping probabilities [66]. Generalization to the case of intelligent predators, i.e. interacting with a prey by means of the long-range potential, may lead to different critical behavior [67, 68, 69]. Simple diffusion processes in power-law small world networks are effectively Lévy flights [70] with the exponent σ controlling the distribution of long-range links. Our work could be used

to understand what network structure, or what σ, would optimize the search and how much more efficient several independent searchers will be.

Chapter 5

Appendix

5.1 Appendix A

Effective four-point function (one-particle irreducible, 1PI) that appeared in (2.25) is composed of usual short-range and new momentum dependent vertices. This gives rise to integrals (2.27). The first integral $\mu = 1$ has been evaluated in [15] by using alpha representation $1/(q^2+s) = \int_0^{+\infty} d\alpha e^{i(q^2+s)\alpha}$ and the result is

$$I_1 = K_d (2s)^{-\varepsilon/2} \Gamma(\varepsilon/2). \tag{5.1}$$

We notice that since there is no angular dependence one can perform $d-1$ integrations and one will be left with one dimensional integral. To compute this integral we use the formula [50]:

$$\int_0^{+\infty} dx \frac{x^{\nu-1}}{P+Qx^2} = \frac{1}{2P} \left(\frac{P}{Q}\right)^{\nu/2} \Gamma\left(\frac{\nu}{2}\right) \Gamma\left(1-\frac{\nu}{2}\right) \tag{5.2}$$

We see that in our case $P = s$, $Q = (D_i + D_j)$ and $\nu = d + (\mu-1)\sigma$. This immediately gives the result:

$$I_\mu = \frac{K_d}{2} \left(\frac{1}{(D_i+D_j)}\right)^{\frac{d+(\mu-1)\sigma}{2}} s^{\frac{d+(\mu-1)\sigma}{2}-1} \times$$

$$\times\Gamma\left(\frac{d+(\mu-1)\sigma}{2}\right)\Gamma\left(1-\frac{d+(\mu-1)\sigma}{2}\right), \tag{5.3}$$

where $K_d = 2^{d-1}\pi^{-d/2}\Gamma^{-1}(d/2)$ is the surface area of d-dimensional unit sphere.

It is convenient to define

$$a_d = \frac{K_d}{2}\left(\frac{2}{(D_i+D_j)}\right)^{d/2}(2s)^{-\varepsilon/2} \tag{5.4}$$

$$b_d = \frac{K_d}{2}\left(\frac{2}{(D_i+D_j)}\right)^{(d+\sigma)/2}(2s)^{-\delta/2} \tag{5.5}$$

$$c_d = \frac{K_d}{2}\left(\frac{2}{(D_i+D_j)}\right)^{(d+2\sigma)/2}(2s)^{-(2\delta-\varepsilon)/2} \tag{5.6}$$

So integral I_μ in the limit of $\delta = O(\varepsilon)$ can be written as:

$$I_1 = \frac{a_d}{\varepsilon}, \quad I_2 = \frac{b_d}{\delta}, \quad I_3 = \frac{c_d}{2\delta-\varepsilon}. \tag{5.7}$$

We used an expansion $\Gamma(\varepsilon/2) \sim 2/\varepsilon$ for small ε. An important property of coefficients (5.4) - (5.6) is that

$$c_d a_d = b_d^2, \tag{5.8}$$

which can be verified by direct substitution.

Now we compute mean field integrals:

$$I_\mu = \int d^d q dt q^{d+\sigma}\exp(-t(D_i+D_j)q^2) \sim t^{-(d+\sigma-2)/2}, \tag{5.9}$$

where we assumed that the large momentum cut-off is imposed and corresponding coupling constants have been renormalized. The non-universal coefficient is not important.

5.2 Appendix B

Here we derive the 1-loop integral

$$I_1 = I_1(\mu) = (2\pi)^{-d} \int d^d k (2\mu + 2k^\sigma)^{-1}. \tag{5.10}$$

We will use dimensional regularization. First we notice that there is no angle dependence under the integral thus one can integrate out $d-1$ angle variable and use alpha representation:

$$X^{-\lambda} = \Gamma(\lambda)^{-1} \int_0^{+\infty} d\alpha \alpha^{\lambda-1} \exp(-\alpha X) \tag{5.11}$$

to handle 1d momenta integral:

$$I_1 = \frac{S_d}{2} \int\limits_0^{+\infty} \frac{k^{d-1} dk}{\mu + k^\sigma} = \frac{S_d}{2} \int\limits_0^{+\infty} \int\limits_0^{+\infty} d\alpha dk k^{d-1} \exp(-\alpha\mu - \alpha k^\sigma) = \frac{S_d}{2\sigma} \Gamma(d/\sigma) \int\limits_0^{+\infty} d\alpha \alpha^{-d/\sigma} \exp(-\alpha\mu), \tag{5.12}$$

where $S_d = 2\pi^{d/2}/\Gamma(d/2)$ is the area of the d-dimensional unit sphere. After taking the integral over α one has

$$I_1 = \frac{S_d}{2\sigma} \Gamma(d/\sigma)\Gamma(\varepsilon/\sigma)\mu^{-\varepsilon/\sigma} = A\mu^{-\varepsilon/\sigma}\varepsilon^{-1} + O(\varepsilon^0), \tag{5.13}$$

where A has been defined by the formula (3.6).

Now we show details of deriving renormalization group flow equations (3.8). We start with equation (3.4) and express λ_{ij} in terms of λ_{Rij}. The result reads

$$\lambda_{ij} = \frac{\lambda_{Rij}}{1 - \lambda_{Rij} I_1}. \tag{5.14}$$

Multiplying left and right hand side of the last equation on $\mu^{-\varepsilon/\sigma}$ and redefining the coupling constant $g_{Rij} = \mu^{-\varepsilon/\sigma}\lambda_{Rij}$ we infer that

$$\mu^{-\varepsilon/\sigma}\lambda_{ij} = g_{Rij}/(1 - g_{Rij} A \varepsilon^{-1}). \tag{5.15}$$

Differentiating left and right hand side of (5.15) with $\mu\frac{\partial}{\partial\mu}$ we obtain

$$(-\varepsilon/\sigma)\mu^{-\varepsilon/\sigma}\lambda_{ij} = -\beta_{ij}g_{Rij}^{-2}/(g_{Rij}^{-1} - A\varepsilon^{-1})^2 \tag{5.16}$$

Now we substitute (5.15) into (5.16) and find beta function up to second order in small ε and g_{Rij} expansion:

$$\beta_{ij} = (-\varepsilon g_{Rij} + Ag_{Rij}^2)/\sigma + O(\varepsilon g^2) \tag{5.17}$$

5.3 Appendix C

Here we derive the 2-loop integral

$$I_2 = I_2(\mu) = (2\pi)^{-2d}\int d^dkd^dq[(2\mu + 2k^\sigma)(3\mu + k^\sigma + q^\sigma + |k+q|^\sigma)]^{-1}. \tag{5.18}$$

The term $|k+q|^\sigma$ leads to the appearance of angle integration. Nevertheless it is possible to avoid angle integration. The key idea is to use Mellin-Barnes representation [63]:

$$\frac{1}{(X+Y)^\lambda} = \int_{-i\infty}^{+i\infty}\frac{dz}{2\pi i}\frac{Y^z}{X^{\lambda+z}}\frac{\Gamma(\lambda+z)\Gamma(-z)}{\Gamma(\lambda)} \tag{5.19}$$

Applying MB formula twice we split the sum of two terms containing q integration into the factor of these terms raised to some power:

$$I_2 = \int\frac{d^dkd^dq}{2(2\pi)^{2d}}\int\limits_{-i\infty}^{+i\infty}\frac{dz}{2\pi i}\frac{\Gamma(1+z_1)\Gamma(-z_1)}{\mu+k^\sigma}\frac{(3\mu+k^\sigma+q^\sigma)^{z_1}}{|k+q|^{\sigma(1+z_1)}}$$

$$= \int\frac{d^dkd^dq}{2(2\pi)^{2d}}\int\limits_{-i\infty}^{+i\infty}\frac{dz_1dz_2}{(2\pi i)^2}\frac{\Gamma(1+z_1)\Gamma(-z_1+z_2)\Gamma(-z_2)}{\mu+k^\sigma}\frac{(3\mu+k^\sigma)^{z_2}}{|k+q|^{\sigma(1+z_1)}q^{\sigma(-z_1+z_2)}}, \tag{5.20}$$

Now integral over q becomes standard:

$$I_q = \int \frac{d^d q}{(q^2)^{a_1}((k+q)^2)^{a_2}} = \pi^{d/2} k^{d-2(a_1+a_2)} \frac{\Gamma(a_1+a_2-d/2)\Gamma(d/2-a_1)\Gamma(d/2-a_2)}{\Gamma(a_1)\Gamma(a_2)\Gamma(d-a_1-a_2)}, \tag{5.21}$$

where $a_1 = \sigma(-z_1+z_2)/2$ and $a_2 = \sigma(1+z_1)/2$. Thus we will be left with integral over k of the form:

$$I_k = \int \frac{d^d k k^{-\varepsilon-\sigma z_2}(3\mu + k^\sigma)}{2\mu + 2k^\sigma} \tag{5.22}$$

The function under the integral does not depend on the angle and therefore I_k can be cast into one dimensional integral over momenta:

$$I_k = \frac{S_d}{2\sigma} \int_0^{+\infty} dk k^{-2\varepsilon/\sigma - z_2} \frac{(3\mu+k)^{z_2}}{\mu+k} \tag{5.23}$$

We will compute this integral using alpha representation.

$$I_k = \frac{S_d}{2\sigma} \int_0^{+\infty} dk d\alpha_1 d\alpha_2 \frac{\alpha_1^{-z_2-1} k^{-2\varepsilon/\sigma - z_2}}{\Gamma(-z_2)} \exp(-3\mu\alpha_1 - \alpha_1 k - \alpha_2 \mu - \alpha_2 k) \tag{5.24}$$

After momenta integration we obtain

$$I_k = \frac{S_d \Gamma(1-2\varepsilon/\sigma - z_2)}{2\sigma\Gamma(-z_2)} \int_0^{+\infty} d\alpha_1 d\alpha_2 (\alpha_1+\alpha_2)^{2\varepsilon/\sigma + z_2 - 1} \alpha_1^{-z_2-1} \exp(-3\mu\alpha_1 - \alpha_2\mu) \tag{5.25}$$

First we will take care the integral over α_2. We do substitution $\tilde{\alpha}_2 = \alpha_1 + \alpha_2$

$$I_k = \frac{S_d \Gamma(1-2\varepsilon/\sigma - z_2)}{2\sigma\Gamma(-z_2)} \int_0^{+\infty} d\alpha_1 \alpha_1^{-z_2-1} e^{-2\mu\alpha_1} \int_{\alpha_1}^{+\infty} d\tilde{\alpha}_2 \tilde{\alpha}_2^{2\varepsilon/\sigma + z_2 - 1} e^{-\tilde{\alpha}_2 \mu}$$

$$= \frac{S_d \Gamma(1-2\varepsilon/\sigma - z_2)\mu^{-z_2-2\varepsilon/\sigma}}{2\sigma\Gamma(-z_2)} \int_0^{+\infty} d\alpha_1 \alpha_1^{-z_2-1} e^{-2\mu\alpha_1} \Gamma(2\varepsilon/\sigma + z_2, \alpha_1\mu), \tag{5.26}$$

where $\Gamma(\lambda, x)$ is incomplete gamma function. The value of the last integral can be found in [50]. The final result or I_k reads

$$I_k = \frac{S_d}{2\sigma}\frac{\Gamma(1-2\varepsilon/\sigma-z_2)}{\Gamma(1-z_2)}\Gamma(2\varepsilon/z_2)\mu^{-2\varepsilon/\sigma}3^{-2\varepsilon/\sigma}\,{}_2F_1(1,2\varepsilon/\sigma,1-z_2,2/3) \qquad (5.27)$$

Inserting (5.21) and (5.27) into (5.20) we infer

$$I_2 = \frac{S_d\pi^{d/2}}{2\sigma(2\pi)^d}\frac{\Gamma(\sigma/2-\varepsilon/2)}{\Gamma(-\varepsilon/\sigma-1)^2}\mu^{-2\varepsilon/\sigma}3^{-2\varepsilon/\sigma}\Gamma(2\varepsilon/\sigma)\int\limits_{-i\infty}^{+i\infty}\frac{dz_1dz_2}{(2\pi i)^2}\,{}_2F_1(1,2\varepsilon/\sigma,1-z_2,2/3)$$

$$\frac{\Gamma(1-2\varepsilon/\sigma-z_2)}{-z_2}\frac{\Gamma(1+z_1)}{\Gamma(\sigma(1+z_1)/2)}\frac{\Gamma(-z_1+z_2)}{\Gamma(\sigma(-z_1+z_2)/2)}\frac{\Gamma(\varepsilon/2+\sigma z_2/2)}{\Gamma(\sigma/2-\varepsilon-\sigma z_2/2)}$$

$$\Gamma(-\varepsilon/2-\sigma z_1/2)\Gamma(-\sigma(-z_1+z_2)/2-\varepsilon/2+\sigma/2). \qquad (5.28)$$

First we sum over all poles of $\Gamma(-\varepsilon/2-\sigma z_1/2)$ and then over pole at $z_2=0$. The result reads

$$I_2 = \frac{S_d\pi^{d/2}}{2\sigma(2\pi)^d}\mu^{-2\varepsilon/\sigma}3^{-2\varepsilon/\sigma}\Gamma(2\varepsilon/\sigma)\,{}_2F_1(1,2\varepsilon/\sigma,1,2/3)\frac{\Gamma(1-2\varepsilon/\sigma)}{\Gamma(\sigma/2-\varepsilon)}\Gamma(\varepsilon/2)$$

$$\sum_{n=0}^{+\infty}\frac{(-1)^n}{n!}\frac{\Gamma(1-\varepsilon/\sigma+2n/\sigma)}{\Gamma(\sigma(1-\varepsilon/\sigma+2n/\sigma)/2)}\frac{\Gamma(\varepsilon/\sigma-2n/\sigma)}{\Gamma(\sigma(\varepsilon/\sigma-2n/\sigma)/2)}\Gamma(-\varepsilon+n\sigma/2). \qquad (5.29)$$

We will look the final result in the form

$$I_2 = \mu^{-2\varepsilon/\sigma}e^{-B\varepsilon}(c_{-2}\varepsilon^{-2}+c_{-1}\varepsilon^{-1}) \qquad (5.30)$$

To obtain the divergent part of I_2 it is convenient to use `MATHEMATICA`. The result for coefficients c_{-2} and c_{-1} are given by the formula (3.18).

5.4 Appendix D

Here we present the derivation of formula (3.20). Expanding scaling function $\ln(Z)$ at two-loop order and [15] one can infer that

$$\ln(Z) = \sum_{1\le i<j\le p} \lambda_{ij} n_i n_j I_1 - \frac{1}{2}\left(\sum_{1\le i<j\le p} \lambda_{ij} n_i n_j I_1\right)^2 - \sum_{1\le i<j\le p} \lambda_{ij}^2 n_i n_j I_1^2$$

$$-\frac{1}{2}\sum_{1\le i<j\le p} \lambda_{ij}^2 n_i^2 n_j^2 I_1^2 + \lambda_{ij}\lambda_{jk} + \lambda_{ik}\lambda_{jk}) n_i n_j n_k I_2$$

$$-\sum_{1\le i<j<k<l\le p} (\lambda_{ij}\lambda_{kl} + \lambda_{ik}\lambda_{jl} + \lambda_{il}\lambda_{jk}) n_i n_j n_k n_l I_1^2 + \frac{1}{2}\sum_{1\le i<j\le p} \lambda_{ij}^2 n_i n_j (n_i + n_j - 2) I_1^2$$

$$+\sum_{1\le i<j<k\le p} (\lambda_{ij}\lambda_{ik} + \lambda_{ij}\lambda_{jk} + \lambda_{ik}\lambda_{jk}) n_i n_j n_k I_1^2 - 2\sum_{1\le i<j<k\le p} (\lambda_{ij}\lambda_{ik}$$

$$-\sum_{1\le i<j<k\le p} (\lambda_{ij}\lambda_{ik} n_i^2 n_j n_k + \lambda_{ij}\lambda_{jk} n_i n_j^2 n_k + \lambda_{ik}\lambda_{jk} n_i n_j n_k^2) I_1^2$$

$$-\sum_{1\le i<j\le p} \lambda_{ij}^2 n_i n_j (n_i + n_j - 2) I_2 + \frac{1}{2}\sum_{1\le i<j\le p} \lambda_{ij}^2 n_i n_j I_1^2. \tag{5.31}$$

By the definition $\gamma = \mu\frac{\partial \ln(Z)}{\partial \mu}$. After differentiation we use the formula $\lambda_{ij}\mu^{-\varepsilon/\sigma} = g_{Rij} + A g_{Rij}^2/\varepsilon$, which one can infer from (5.15), and the integral expansions (3.18) and

$$I_1^2 = \frac{2^{-2\sigma}\pi^{-\sigma}}{\varepsilon^2 \Gamma(\sigma/2)^2} + \frac{2^{-2\sigma}\pi^{-\sigma}}{\varepsilon \Gamma(\sigma/2)^2}[\ln(4\pi) + \psi^{(0)}(\sigma/2)] + O(\varepsilon^0) \tag{5.32}$$

to derive the following result

$$\gamma = -\frac{1}{\sigma}\sum_{1\le i<j\le p} n_i n_j g_{Rij} - \frac{1}{\varepsilon\sigma}\sum_{1\le i<j\le p} n_i n_j g_{Rij}^2 + \frac{2}{\varepsilon\sigma}\sum_{1\le i<j\le p} n_i n_j g_{Rij}^2 - \frac{1}{\varepsilon\sigma}\sum_{1\le i<j\le p} n_i n_j g_{Rij}^2$$

$$+\sum_{1\le i<j<k\le p} n_i n_j n_k (g_{Rij}g_{Rik} + g_{Rij}g_{Rjk} + g_{Rik}g_{Rjk}) \left(\frac{2}{\sigma^2}\frac{2^{-2\sigma}\pi^{-\sigma}}{\Gamma(\sigma/2)^2}\ln(3/4)\right)$$

$$+\sum_{1\le i<j\le p} g_{Rij}^2 n_i n_j (n_i + n_j - 2) \left(\frac{1}{\sigma^2}\frac{2^{-2\sigma}\pi^{-\sigma}}{\Gamma(\sigma/2)^2}\ln(3/4)\right). \tag{5.33}$$

The critical exponent is the value of this expression evaluated at the fixed point $g_{Rij} = \varepsilon$. It easy to see that the resut is equivalent to (3.20).

References

[1] U. C. Tauber, M. Howard and B. P. Vollmayr-Lee, J.Phys. **A38** R79 (2005).

[2] H. Zhu, J. Y. Zhu, Phys. Rev. E **66**, 017102 (2002).

[3] D. S. Fisher, Phys. Rev. Lett. **56**, 416 (1986).

[4] K. G. Wilson, Rev. Mod. Phys. **47**, 773 (1975).

[5] P. C. Hohenberg and B. I. Halperin, Rev. Mod. Phys. **49**, 435 (1977).

[6] S. C. Park, D. Kim and J. M. Park, Phys. Rev. E **62**, 7642 (2000).

[7] D. Brockmann, L. Hufnage and T. Geisel, Nature **439**, 462 (2006).

[8] M. A. Lomholt, B. van den Broek, S.-M. J. Kalisch, G. J. L. Wuite and R. Metzler, PNAS **106**, 8204 (2009).

[9] P. Barthelemy, J. Bertolotti and D. S. Wiersma, Nature **453**, 495 (2008).

[10] M. Doi J. Phys. A: Math. Gen. **9** 1465 (1976).

[11] M. Peliti J. Physique **46** 1469 (1985).

[12] D. Vernon and M. Howard, Phys. Rev. E **63**, 041116 (2001); arXiv:cond-mat/0011475.

[13] L. Chen and M. W. Deem, Phys. Rev. E **65**, 011109 (2001); cond-mat/0107158.

[14] M. E. Fisher, J. Stat. Phys. **34**, 667 (1984).

[15] J. Cardy and M. Katori, J. Phys. A **36**, 609 (2003).

[16] B. J. Reynwar *et al*, Nature **447** 461 (2007).

[17] B. J. Reynwar and M. Deserno, Biointerphases **3** FA117 (2008).

[18] K. Simons and E. Ikonen, Nature **387**, 569 (1997).

[19] G. Guigasa and M. Weiss, Biophys. J. **91**, 2393 (2006).

[20] L. Valkunas, Y. Z. Ma and G. R. Fleming, Phys. Rev. B **73**, 115432 (2006).

[21] R. H. Baughman, A. A. Zakhidov and W. A. de Heer, Science **297**, 787 (2002).

[22] D. W. Sims *et al*, Nature **451**, 1098 (2008).

[23] G. Ramos-Fernandez, J. L. Mateos, O. Miramontes, G. Cocho, H. Larralde and B. Ayala-Orozco, Behav. Ecol. Sociobiol. **55**, 223 (2004).

[24] D. J. Amit, *Field Theory, the Renormalization Group and Critical Phenomena*, (World Scientific, Singapore, 1984).

[25] J. Zinn-Justin, *Phase Transitions and Renormalization Group*, (Oxford University Press, Oxford, 2007).

[26] C. A. Angell Science **267** 1924 (1995).

[27] D. S. Dean and A. Lefevre, Phys. Rev. E (2004).

[28] D. R. Nelson and P. Le Doussal Phys. Rev. B **42** 10113 (1990).

[29] M. Nakamura *et al* Phys. Rev. B **49** 16191 (1993).

[30] C. Kane, L. Balents and M. P. A. Fisher Phys. Rev. Lett. **79** 5086 (1997).

[31] J. M. Park and M. W. Deem Euro. Phys. J. *ArXiv: cond-mat/9811102*.

[32] J. Klafter and J. Jortner J. Chem. Phys. **73** 1004 (1980).

[33] V. Kuzovkov and E. Kotomin, Rep. Prog. Phys. 51, 1479 (1988).

[34] S. Redner, P. L. Krapivsky, Am. J. Phys. **67**, 1277 (1999).

[35] P. L. Krapivsky and S. Redner J. Phys. A **29** 5347 (1996).

[36] A. J. Bray and R. A. Blythe Phys. Rev. Lett. **89** 150601 (2002).

[37] S. Mukherji and S. M. Bhattacharjee Phys. Rev. E **48** 3427(1993); Erratum Phys. Rev. E **52** 3301 (1995).

[38] S. Mukherji and S. M. Bhattacharjee J. Phys. A: Math. Gen. **26** L1139 (1993).

[39] B. Derrida and M. R. Evans J. Phys. A: Math. Gen. **32** 4833 (1999) *arXiv:cond-mat/9902133*.

[40] A. Weinrib and B. I. Halperin Phys. Rev. B **27** 413 (1983).

[41] V. Blavats'ka *et al* Phys. Rev. E **64** 041102 (2001).

[42] V. V. Prudnikov *et al* Phys. Rev. B **62** 8777 (2000).

[43] H. J. Schulz Phys. Rev. Lett. **71** 1864 (1993).

[44] A. Mironov and A. Zabrodin Phys. Rev. Lett. **66** 534 (1991).

[45] F. Linder *et al* J. Phys. A: Math. Theor. **41** 185005 (2008) *arXiv:0802.1028*.

[46] M. Katori, H. Tanemura, Phys. Rev. E **66**, 011105 (2002).

[47] S. Mukherji and S. M. Bhattacharjee Phys. Rev. E **63** 051103 (2001); Erratum **64** 059902 (2001); *arXiv:cond-mat/0101128*.

[48] G. D. Mahan *Many-particle physics* (Plenum, 1993).

[49] A. L. Fetter and J.D. Walecka *Quantum theory of many-particle systems* (McGraw-Hill, 2003).

[50] I. S. Gradshtein I. M. Ryjik *Tables of Integrals*, (Academic Press, 1965).

[51] M. F. Shlesinger, B. J. West and J. Klafter, Phys. Rev. Lett. **58**, 1100 (1987).

[52] N. Menyhard and G. Odor J. Phys. A: Math. Gen. **28**, 4505 (1995).

[53] B. Bergersen and Z. Rácz, Phys. Rev. Lett. **67**, 3047 (1991).

[54] R. Metzler and J. Klafter, Phys. Rep. **339**, 1 (2000).

[55] G. M. Viswanathan, V. Afanasyev, S. V. Buldyrev, E. J. Murphy, P. A. Prince and H. E. Stanley Nature **381**, 413 (1996).

[56] P. Barthelemy, J. Bertolotti and D. S. Wiersma, Nature **453**, 495 (2008).

[57] E. Katzav, Phys. Rev. E **68**, 031607 (2003); cond-mat/0303178.

[58] A. Ott, J. P. Bouchaud, D. Langevin, and W. Urbach, Phys. Rev. Lett. **65**, 2201 (1990).

[59] M. F. Shlesinger, Nature **411**, 641 (2001).

[60] H. K. Janssen and O. Stenull, Phys. Rev. E **78**, 061117 (2008).

[61] H. Hinrichsen, J. Stat. Mech.: Theor. Exp. P07066 (2007).

[62] J. B. Bronzan and J. W. Dash, Phys. Rev. D **10**, 4208 (1974).

[63] V. A. Smirnov, *Evaluating Feynman Integrals*, (Springer, 2004).

[64] R. Metzler and J. Klafter, J. Phys. A **37**, R161 (2004).

[65] F. Bartumeus, J. Catalan, U. L. Fulco, M. L. Lyra, and G. M. Viswanathan, Phys. Rev. Lett. **88**, 097901 (2002).

[66] R. F. Kayser and J. B. Hubbard Phys. Rev. Lett. **51**, 79 (1983)

[67] I. Goncharenko and A. Gopinathan, arXiv:1003.5970.

[68] G. Schehr, S. N. Majumdar, A. Comtet and J. Randon-Furling, Phys. Rev. Lett. 101, 150601 (2008).

[69] C. Nadal and S. N. Majumdar, Phys. Rev. E **79**, 061117 (2009).

[70] B. Kozma, M. B. Hastings and G. Korniss, Phys. Rev. Lett. **95**, 018701 (2005).